Supplementary Information (SI) for RSC Advances.
This journal is © The Royal Society of Chemistry 2025

SUPPORTING INFORMATION

Self-Assembled Isomorphous 2D Triangular Networks: Divergent Magnetic Relaxation in Co(II) and Cu(II)

Luckerman D. G. Botelho,[a] Henrique C. S. Junior,[b] Guilherme P. Guedes,[c] Davor L. Mariano,[d] Angelo M. Gomes,[d] Wallace C. Nunes,[e*] Maria Vanda Marinho.[a*]

[a]Instituto de Química, Universidade Federal de Alfenas, Campus Santa Clara, Alfenas, MG, 37133-840, Brazil. maria.marinho@unifal-mg.edu.br

[b]Departamento de Química Fundamental, Instituto de Química, Universidade Federal Rural do Rio de Janeiro, Seropédica, RJ, 23890-000, Brazil.

[c]Instituto de Química, Universidade Federal Fluminense, Niterói, Rio de Janeiro, RJ 24020-141, Brazil.

[d]Instituto de Física, Universidade Federal do Rio de Janeiro, Cidade Universitária, Rio de Janeiro 21941-972, Brazil.

[e]Instituto de Física, Universidade Federal Fluminense, Rio de Janeiro, RJ 24210-346, Brazil. wcnunes@id.uff.br

Table S1. Summary of cobalt(II) and copper(II) compounds exhibiting SIM or SMM behavior, compiled from an extensive literature survey.

Formula	Nature	Geometry	External field (kOe)	U_{eff}/K_B (K)	τ_0 (s)	D(cm^{-1})	Magnetic behavior	Effect	Ref.
$[Co_4(phen)_4Cl_8]$	Complex	Distorted octahedral	--	8.41	$5.29x10^{-7}$	--	SMM	QTM	1
$[Co_4(phen)_4Cl_8]$	Complex	Distorted octahedral	1.0	14.04	$2.87x10^{-8}$	--	SMM	QTM	1
dmphCoBr	Complex	Distorted tetrahedron	1.0	22.8(8)	$3.7(5)x10^{-10}$	10.62	SMM	Orbach	2
$[Co(biq)Cl_2]$	Complex	Distorted tetrahedron	2.0	42.6(5)	$1.9(3)x10^{-10}$	10.5	SMM	Direct Orbach	3
$[Co(biq)Cl_2]$	Complex	Distorted tetrahedron	3.0	41.2(13)	$3.0(12)x10^{-10}$	10.5	SMM	Direct Orbach	3
$[Co(biq)Br_2]$	Complex	Distorted tetrahedron	2.0	39.6(91)	$1.2x10^{-10}$	12.5	SMM	Direct Orbach	3
$[Co(biq)Br_2]$	Complex	Distorted tetrahedron	3.0	42.3(6)	$5.0(9)x10^{-11}$	12.5	SMM	Direct Orbach	3
$[Co(biq)I_2]$	Complex	Distorted tetrahedron	2.0	57.0(7)	$3.2(6)x10^{-13}$	10.3	SMM	Direct Orbach	3
$[Co(biq)I_2]$	Complex	Distorted tetrahedron	3.0	38.7(37)	$9.9(9)x10^{-11}$	10.3	SMM	Direct Orbach	3
$C_{16}H_{52}B_{20}N_2S_4Co$	Complex	Distorted tetrahedral	--	38.5(6)	$3.3x10^{-6}$	-71.6	SMM	QTM Raman	4
$[Co(dmphen)Br_2]$	Complex	Distorted tetrahedron	2.0	64.5(41)	$6.8(75)x10^{-14}$	13.8	SMM	Orbach Direct QTM	5
$[Co(dmphen)Br_2]$	Complex	Distorted tetrahedron	4.0	35.0(50)	$3.0(41)x10^{-10}$	13.8	SMM	Orbach Direct QTM	5
$[Co(dmphen)I_2]$	Complex	Distorted tetrahedron	2.0	69.6(30)	$2.1(18)\ x10^{-14}$	16.6	SMM	Orbach Direct QTM	5

$[Co(dmphen)I_2]$	Complex	Distorted tetrahedron	4.0	41.5(41)	$0.64(70)x10^{-10}$	16.6	SMM	Orbach Direct QTM	5
$[Co(NS_3^{tBu})NCS]ClO_4$	Complex	Trigonal bipyramidal	--	20	$2.0x10^{-9}$	-11	SMM	Direct Raman	6
$[Co(N_3)L^{1*}H_3]Cl_4$	Complex	Trigonal bipyramidal	0.5	21.58(2)	$5.0x10^{-9}$	-7.1	SMM	Orbach	7
$[Co_4(mbm)_4Br_4-(CH_3OH)_4]$	Complex	Distorted octahedral	--	26.7	$1.3x10^{-9}$	--	SMM	QTM	8
$[Co_4(mbm)_4Br_4-(CH_3OH)_4]$	Complex	Distorted octahedral	0.75	26.7	$1.3x10^{-9}$	--	SMM	QTM	8
$[Co_4(mbm)_4Br_4-(CH_3CH_2OH)_4]$	Complex	Distorted octahedral	--	21	$9.7x10^{-9}$	--	SMM	QTM	8
$[Co_4(mbm)_4Br_4-(CH_3CH_2OH)_4]$	Complex	Distorted octahedral	0.75	26	$5.6x10^{-9}$	--	SMM	QTM	8
$[Co_3(Himn)_6]Cl_2\cdot 2CH_3OH$	Complex	Trigonal antiprism	--	58.99	$6.76x10^{-8}$	-112.0	SMM	Raman Orbach	9
$[Co^{II}(L^{2*})_2](DPAS)_2\cdot DMF$	Complex	Distorted octahedral	1.0	34.1	$2.1x10^{-7}$	-75.1(8)	SMM	Raman Direct	10
$[Co^{II}(bppCOOH)_2](ClO_4)_2\cdot 2Me_2CO$	Complex	Distorted octahedral	--	15.9	$2.7x10^{-6}$	51.6	SMM	Raman	11
$[Co(H_2daps)(MeOH)_2]$	Complex	Pentagonal bipyramidal	1.0	33.5	$7.4x10^{-6}$	43.1(7)	SMM	QTM Raman	12
$[Co(H_4daps)(NCS)(MeOH)]\cdot(ClO_4)\cdot(MeOH)$	Complex	Pentagonal bipyramidal	1.0	28.4	$5.6x10^{-6}$	41.5(6)	SMM	QTM Raman	12
$[Co(H_4daps)(NCS)_2]\cdot(MeOH)_2$	Complex	Pentagonal bipyramidal	1.0	23.6	$4.8x10^{-6}$	38.8(2)	SMM	QTM Raman	12
$[Co(abpt)_2(N_3)_2]$	3D Supramolecular network	Distorted octahedral	--	29	$7.7x10^{-7}$	-24.1	SMM	Direct Raman Orbach	13
$[Co(half\text{-}Pc)_2]$	Complex	Pseudotetra-hedral	--	77.7(7)	$3.17x10^{-10}$	-27.9	SMM	Orbach	14

$[Co(pyterpy)(NO_3)_2]$	1D Complex	Octahedral	1.0	4.24	$3.02x10^{-5}$	70.4	SMM	Orbach	15
$[CoL_{diProp}(CH_3CN)](ClO_4)_2$	Complex	Trigonal prismatic	--	13(1)	$4.3(12)x10^{-6}$	-25.8	SMM	Orbach Direct	16
$[Co(tppz)_2][Co_2(H_2mpba)_3]\cdot 9H_2O$	Complex	Octahedral	1.0	17.8(2)	$3.2(1)\ x10^{-7}$	79.2	SMM	Direct Raman	17
$[Co(tppz)_2][Co_2(H_2mpba)_3]\cdot 9H_2O$	Complex	Octahedral	2.0	14.4(1)	$6.5(1)x10^{-7}$	79.2	SMM	Direct Raman	17
$[Co(L^{3*})](ClO_4)_2\cdot 2CH_3OH$	Complex	Trigonal prismatic	--	38.6(7)	$1.7(1)x10^{-6}$	-116.6(6)	SMM	Raman QTM	18
$[Co(L^{3*})](BF_4)_2\cdot 2CH_3OH$	Complex	Trigonal prismatic	--	39.2(4)	$1.85(5)x10^{-6}$	-127.6(8)	SMM	Raman QTM	18
$[Co(L^{3*})(SCN)_2]$	Complex	Distorted octahedral	--	10.30(7)	$1.2(2)x10^{-5}$	34.7(1)	SMM	Direct QTM	18
$[Co(3C_{16}bzimpy)_2](BF_4)_2$	Complex	Octahedral	1.0	7.0(66)	$2.5x10^{-5}$	49.65	SMM	Orbach	19
$[\{(PyPz_3)Co\}_2(dhbq)][PF_6]_2$	Complex	Trigonal prismatic	--	97(3)	$7.8(1)x10^{-8}$	-78.5	SMM	QTM Orbach Raman	20
$[\{(PyPz_3)Co\}_2(dhbq)][PF_6]_2$	Complex	Trigonal prismatic	1.0	124(6)	$2.0(4)x10^{-11}$	-78.5	SMM	QTM Orbach Raman	20
$[Co(CH_3COO)_2(C_2H_5N)_2(H_2O)_2]$	Complex	Pseudo-octahedral	1.5	25.0	$6.7x10^{-7}$	--	SMM	Orbach	21
$[Co(bzpy)_4(NCS)_2]$	Complex	Distorted tetragonal bipyramidal	2.0	22.9	$1.16x10^{-6}$	90.5	SMM	Orbach	22
$[Co(bzpy)_4(NCS)_2]$	Complex	Distorted tetragonal bipyramidal	4.0	27.7	$0.31x10^{-6}$	90.5	SMM	Orbach	22
$[Co(4\text{-}HOpa)_2(H_2O)_2]$	Complex	Distorted octahedral	1.0	46	--	71.35	SMM	Bottleneck Raman	23
α-$[Co(3,5\text{-}Hdnb)_2(py)_2$	Complex	Distorted	1.0	28.1(6)	$1.37x10^{-7}$	58	SIM	Direct	24

$(H_2O)_2]$		octahedral						Raman	
β-$[Co(3,5\text{-}Hdnb)_2(py)_2(H_2O)_2]$	Complex	Octahedral	1.0	30.3(9)	$3.4x10^{-8}$	68	SIM	Direct Raman	24
$[Co(pydm)_2](dnbz)_2$	Complex	Distorted tetragonal bipyramid	--	44.1(8)	$2.8(4)x10^{-9}$	44	SIM	QTM Raman	25
$\{[Co(bmzbc)_2]\cdot 2DMF\}_n$	3D Metal-organic framework	Octahedral	--	11.8	$1.3x10^{-5}$	53.2	SIM	QTM	26
$[Co(bpeb)_2(NCS)_2]\cdot 7DCB$	2D Metal-organic framework	Distorted octahedral	0.25	43.06	$0.23x10^{-7}$	64.9(9)	SIM	Orbach Raman	27
$[Co(bpeb)_2(NCS)_2]\cdot 7DCB$	2D Metal-organic framework	Distorted octahedral	0.5	42.05	$0.27x10^{-7}$	64.9(9)	SIM	Orbach Raman	27
$[Co(bpeb)_2(NCS)_2]\cdot 7DCB$	2D Metal-organic framework	Distorted octahedral	1.0	45.07	$0.17x10^{-7}$	64.9(9)	SIM	Orbach Raman	27
$[Co(bpeb)_2(NCS)_2].4TAN.4MeOH$	2D Metal-organic framework	Distorted octahedral	1.0	24.62	$2.27x10^{-7}$	67.1(9)	SIM	Orbach Raman	27
$[Co(bpeb)_{2(}NCS)_2].6TOL$	2D Metal-organic framework	Distorted octahedral	1.0	16.56	$8.22x10^{-7}$	84.4(4)	SIM	Orbach Raman	27
$[Co(bpeb)_2(NCS)_2].8PYR$	2D Metal-organic framework	Distorted octahedral	1.0	30.24	$1.30x10^{-7}$	70.3(9)	SIM	Orbach Raman	27
$[Co(tdmmb)(bpe)][BF_4]_2\cdot 2CH_3CN$	1D Coordination polymer	Distorted pentagonal bipyramidal	1.0	19	$7.5x10^{-6}$	21.7(7)	SIM	QTM	28
$Et_4N[Co^{II}(hfac)_3]$	Complex	Distorted octahedral	0.0	18(2)	$9(5)x10^{-6}$	117.8	SIM	Direct Raman Orbach	29
$Et_4N[Co^{II}(hfac)_3]$	Complex	Distorted octahedral	1.0	20.6(5)	$6.4(9)x10^{-6}$	117.8	SIM	Direct Raman Orbach	29
$[Co(bmim)_2(SCN)_2]$	Complex	Distorted tetrahedral	0.5	22.03	$2.15x10^{-9}$	-7.5	SIM	Orbach	30
$[Co(bmim)_2(SCN)_2]$	Complex	Distorted	1.0	22.46	$2.08x10^{-9}$	-7.5	SIM	Orbach	30

		tetrahedral							
$[Co(bmim)_2(SCN)_2]$	Complex	Distorted tetrahedral	2.5	5.20	$3.61x10^{-9}$	-7.5	SIM	Orbach	30
$[Co(bmim)_2(NCO)_2]$	Complex	Distorted tetrahedral	1.0	15.55	$6.80x10^{-9}$	6.3	SIM	Orbach	30
$[Co(bmim)_2(NCO)_2]$	Complex	Distorted tetrahedral	2.5	13.97	$1.70x10^{-8}$	6.3	SIM	Orbach	30
$[Co(bmim)_2(N_3)_2]$	Complex	Distorted tetrahedral	1.0	9.61	$2.5x10^{-8}$	6.7	SIM	Orbach	30
$[Co(bmim)_2(N_3)_2]$	Complex	Distorted tetrahedral	2.5	10.81	$3.20x10^{-8}$	6.7	SIM	Orbach	30
$[Co(L^{4*})_2Cl_2]$	Complex	Distorted tetrahedral	1.2	26.2	$3.69x10^{-10}$	-18.1	SIM	Orbach	31
$[Co(L^{4*})_2Br_2]$	Complex	Distorted tetrahedral	2.75	22.9	$2x10^{-8}$	-16.4	SIM	QTM Raman Orbach	31
$[Co(L^{4*})_2I_2]$	Complex	Distorted tetrahedral	1.7	27.8	$1.22x10^{-8}$	-22.0	SIM	QTM Raman Orbach	31
$[Co^{II}(L^{5*})_2](ClO_4)_2$	Complex	Distorted triangular dodecahedron	0.5	44	$7.4x10^{-9}$	-29.4	SIM	Orbach Raman	32
$[Co^{II}(L^{6*})_2](ClO_4)_2$	Complex	Distorted triangular dodecahedron	0.5	20	$3.9x10^{-9}$	-40.5	SIM	Orbach Raman	32
$[Co^{II}(L^{7*})_2](ClO_4)_2$	Complex	Distorted triangular dodecahedron	0.5	18	$2.3x10^{-7}$	-22.0	SIM	Orbach Raman	32
$[Co^{II}(L^{8*})_2](ClO_4)_2$	Complex	Distorted triangular dodecahedron	0.5	31	$3.9x10^{-9}$	-15.8	SIM	Orbach Raman	32
$\{[Co_2(dmphen)_2(CPCA)_2]DMF\}$	1D Coordination polymer	Distorted trigonal	5.0	9.2	$9.1x10^{-5}$	38.2(4)	SIM	QTM Orbach	33

		prismatic							
$[Co(C_{10}\text{-terpy})_2](BF_4)_2$	Complex	Distorted octahedral	1.0	13.8(9)	$1.1(4)\times10^{-5}$	47.5	SIM	Orbach Raman	34
$[Co(dmphen)_2(OOCPh)]ClO_4\cdot 0.5H_2O\cdot 1/2CH_3OH$	Complex	Distorted octahedral	0.5	9.80(14)	$1.62(10)\times10^{-6}$	61.9	SIM	Orbach	35
$[Co(dmphen)_2(OOCPh)]ClO_4\cdot 1/2H_2O\cdot 1/2CH_3OH$	Complex	Distorted octahedral	1.0	8.89(16)	$4.2(3)\times10^{-6}$	61.9	SIM	Orbach	35
$[Co(dmphen)_2(OOCPh)]ClO_4\cdot 1/2H_2O\cdot 1/2CH_3OH$	Complex	Distorted octahedral	2.5	6.92(15)	$11.5(8)\times10^{-6}$	61.9	SIM	Orbach	35
$[Co(dmbipy)_2(OOCPh)]ClO_4$	Complex	Distorted octahedral	0.5	8.52(11)	$1.44(7)\times10^{-6}$	61.6	SIM	Orbach	35
$[Co(dmbipy)_2(OOCPh)]ClO_4$	Complex	Distorted octahedral	1.0	9.47(7)	$1.42(4)\times10^{-6}$	61.6	SIM	Orbach	35
$[Co(dmbipy)_2(OOCPh)]ClO_4$	Complex	Distorted octahedral	2.5	10.08(13)	$1.45(7)\times10^{-6}$	61.6	SIM	Orbach	35
$[Co^{II}(BPA\text{-}TPA)](BF_4)_2$	Complex	Capped trigonal prismatic	1.0	39.7	1.53×10^{-9}	21.4	SIM	Orbach Raman	36
$[CoL^{9*}(NCS)_2]\cdot DMSO$	Complex	Distorted prismatic trigonal	1.0	35.6(9)	$2.5(2)\times10^{-5}$	-1538.0	SIM	Orbach	37
[Co(N,N'-2-iminopyrrolyl)$_2$]	Complex	Tetrahedral	--	85	$2.1(1)\times10^{-9}$	-42.6(4)	SIM	Orbach Raman	38
$Co(H_2DPA)\cdot 2H_2O$	Complex	Distorted octahedral	1.5	43.28	2.11×10^{-8}	67.63(22)	SIM	Direct Raman	39
$[Co(btca)_{1/2}(mbpy)]_n$	1D Coordination polymer	Distorted trigonal bipyramidal	1.0	29.1	3.4×10^{-7}	-37.2	SIM	QTM Raman	40
$\{[Co(H_2tbca)(bpb)(H_2O)_2]\cdot bpb\}_n$	2D Metal-organic framework	Distorted octahedral	--	31.8	--	62.1	SIM	Direct Raman	41

$[L^{10*}{}_2Co](TBA)_2$	Complex	Distorted tetrahedral	--	325	1.46x10-^{10}	-113.0	SIM	Orbach Raman	42
$[Co(CzPh_2PO)_2Cl_2]$	Complex	Distorted tetrahedral	1.0	28.9	$2.51x10^{-9}$	-16.4	SIM	Orbach	43
$[Co(CzPh_2PO)_2Br_2]$	Complex	Distorted tetrahedral	1.0	22.7	$5.19x10^{-9}$	-13.8	SIM	Orbach	43
$[Co(CzPh_2PO)_2I_2]$	Complex	Distorted tetrahedral	0.8	60.9	$2.05x10^{-9}$	14.6	SIM	Orbach	43
$[Co(bcpp)Cl_2]$	Complex	Trigonal bipyramid	2.0	11.2	$8.6x10^{-6}$	64.68	SIM	Raman	44
$[Co(bcpp)Br_2]$	Complex	Trigonal bipyramid	2.0	5.59	$7.22x10^{-3}$	45.00	SIM	Raman	44
$[Co(12\text{-}TMC)(NCS)_2]\cdot 0.5CH_3OH$	Complex	Distorted octahedral	6.0	23.23	$3.0x10^{-8}$	32.10(0)	SIM	Orbach	45
$[Co(12\text{-}TMC)(N(CN)_2)_2]$	Complex	Distorted octahedral	2.0	27.31	$1.14x10^{-8}$	25.95(9)	SIM	Orbach Raman	45
$[Co(12\text{-}TMC)(NCO)][B(C_6H_5)_4$	Complex	Distorted square pyramidal	2.0	23.16	$1.17x10^{-9}$	--	SIM	Orbach Raman	45
$[Co(dca)_2(atz)_2]_n$	2D Coordination polymer	Elongated octahedral	1.0	5.1	$1.7x10^{-6}$	--	SIM	Orbach	46
$[Co(L^{11*})_2(SCN)_2\cdot 2(CH_3CN)\cdot 2(dmf)]_n$	2D Coordination polymer	Distorted octahedral	1.0	36.9	$1.4x10^{-6}$	41.6	SIM	QTM Raman	47
$[Co(ppad)_2]_n$	2D Coordination polymer	Distorted octahedral	2.0	11.37	$5.03x10^{-6}$	76	SIM	Orbach	48
cis-$[Co(dmphen)_2(NCS)_2]\cdot 0.25EtOH$	Complex	Distorted octahedral	1.0	23.33	$4.37x10^{-7}$	98	SIM	Orbach	49
cis-$[Co(dmphen)_2(NCS)_2]\cdot 0.25EtOH$	Complex	Distorted octahedral	2.5	26.06	$3.03x10^{-7}$	98	SIM	Orbach	49
cis-$[Co(dmphen)_2(NCS)_2]\cdot 0.25EtOH$	Complex	Distorted octahedral	5.0	23.90	$4.02x10^{-7}$	98	SIM	Orbach	49
$[Co(dps)_2Cl_2]$	2D Complexes	Distorted	1.5	11.0	$2.38x10^{-5}$	27.2(1)	SIM	Orbach	50

		octahedral						Raman	
$[Co(dps)_2Br_2]_n$	2D Complexes	Distorted octahedral	1.5	28.9	$7.40x10^{-7}$	28.0(9)	SIM	QTM Direct	50
$[Co(dps)_2(H_2O)_2 \cdot I_2 \cdot (H_2O)_4]_n$	2D Complexes	Distorted octahedral	1.5	25.3	$5.54x10^{-7}$	9.5(5)	SIM	QTM Direct	50
$\{[Co(H_3BTB)_2(phen)](NO_3)_2\}_n$	1D Coordination polymer	Distorted octahedral	2.0	12.1(3)	$5.52(4)x10^{-7}$	74.7(3)	SIM	QTM Direct	51
$[Co_2(H_2mpba)_2(H_2O)_4]_n \cdot 4nH_2O$	Coordination polymer	Distorted octahedral	2.0	110(10)	$1.3(0.1)x10^{-10}$	79.0	SIM	Orbach	52
$[Co(dca)_2(bim)_4]$	Complex	Distorted octahedral	2.5	7.74	0.87×10^{-6}	69.6	SIM	Raman Orbach	53
$[Co(dca)_2(bim)_2]_n$	Coordination polymer	Distorted octahedral	2.5	5.33	1.54×10^{-6}	74.3	SIM	Orbach	53
$[Co(dca)_2(bmim)_2]_n$	Coordination polymer	Distorted octahedral	2.5	13.81	0.63×10^{-6}	75.8	SIM	Orbach	53
$[\{Co(H_2mpba)(dps)\}.2DMSO]_n$	2D Coordination polymer	Distorted octahedral	--	--	--	-103.7(7)	SIM	Bottleneck	This work
$[\{Co(H_2mpba)(dps)\}.2DMSO]_n$	2D Coordination polymer	Distorted octahedral	1.0	56(3)	$1.2(1)x10^{-8}$	-103.7(7)	SIM	Bottleneck Orbach	This work
$[\{Cu(H_2mpba)(dps)\}.2DMSO.H_2O]_n$	2D Coordination polymer	Distorted octahedral	1.0	--	--	--	SIM	Bottleneck	This work

phen= 1,10-phenanthroline; **dmph**= 2,9-dimethyl-1,10-phenanthroline; **biq**= 2,2'-biquinoline; **dmphen**= 2,9-dimethyl-1,10-phenantroline; **NS_3^{tBu}**= 2-(tert-butylthio)-N-(2-(tert-butylthio)ethyl)-N-((neopentylthio)methyl)ethan-1-amine; **L^{1*}**= 6,16,2,5-tribenzena(1,4) 1,4,8,11,14,18,23,27-octaazabicyclo[9.9.9]nonaco-saphane; **L^{C14}**= 4-tetradec-1-ynyl-2,6-di-pyrazol-1-yl-pyridine; **mbm**= 1-Me-(1H-benzo[d]imidazol-2-yl)methanolate; **$Himn^-$**= 2-(2-imidazolinyl)phenolate); **L^{2*}**= 4' (4 Bromophe-nyl)2,2':6',2" terpyridine; **DPAS**= 4(phenylamino) benzenesulfonate; **bppCOOH**= 2,6-Di(1H-pyrazol-1-yl)isonicotinic acid; **H_4daps**= 2,6-bis(1-salicyloylhy-drazonoethyl)pyridine; **abpt**= 4-amino-3,5-bis(pyridin-2-yl)-1,2,4-triazole); **half-Pc**= (Z)-1-((1,1-dimethoxy-1H-isoindol-3-yl)imino)-3-iminoisoindolin-2-ide; **pyterpy**= 4′-(4‴-pyridyl)-2,2′:6′2″-terpyridine; **L_{diProp}**= (1,5,13,17,22 pentaazatricyclo-[15.2.2.17,11]docosa-7,9,11(22)-triene); **tppz** = 2,3,5,6 tetrakis(2-pyridyl)pyrazine; **H_4mpba**= 1,3-phenylenebis(oxamic) acid); **L^{3*}**= tris(pyridylhydrazonyl)phos-phorylsulfide; **$3C_{16}$-bzimpy**= 2,2'-(4-hexade cyloxy-2,6-diyl)bis(1-hexadecyl-1H-benzo[d]imidazole); **dhbq**= 2,5-dioxo-1,4-benzoquinone; **bzpy**= 4 benzylpyridine; **4-HOpa**= N-4-hydroxyphenyloxamate; **3,5-Hdnb**= 3,5-dinitrobenzoic acid; **py**= pyridine; **pydm**= 2,6pyridinedimethanol; **dnbz**= 3,5dinitrobenzoato; **bmzbc**= 4-(benzimidazole-1-yl)benzoate; **bpeb**= 1,4-bis(4'-Pyridylethynyl)benzene(bpeb); **DCB**= ortho-dichlorobenzene; **TAN**= thianthrene; **TOL**= toluene; **PYR**= pyrrole; **tdmmb**= 1,3,10,12-tetramethyl-1,2,11,12-tetra-aza[3](2,6)pyridino[3](2,9)-1,10-phenanthrolinophan-2,10-diene; **bpe**= 1,2-di(4-pyridyl)ethane; **hfac**= hexafluoro-acetylacetonate; **bmim**= 1-benzyl-2-methylimidazole; **L^{4*}**= Tetramethylthiourea; **$L^{5*=}$** Dimethyl-1,10-phenanthroline-2,9-carboxylate; **$L^{6*=}$** Dibutyl-1,10-phenanthroline-2,9-carboxylate; **$L^{7*=}$** Dimethyl[2,2'-bipyridine]-6,6'-dicarboxylate; **$L^{8*=}$** Dibutyl[2,2'-bipyridine]-6,6'-dicarboxylate; **H_2CPCA**= 3-(3-carboxyphenyl)-1H-pyra zole-5-carboxylic acid; **C_{10}-terpy**= 4′-alkoxy-2,2':6′,2″-terpyridine; **HOOCPh**= benzoic acid;

dmbipy= 6,6′-dimethyl-2,2′-bipyridine; **BPA-TPA**= [2,6-bis[bis(2pyridylmethyl)amino]-methyl]pyridine; **L**^{9*}= 2,2′-((Butane-2,3-diylidene)-bis(hydrazin-1-yl-2-ylidene))bis (4,6-dimethylpyrimidine); **iminopyrrolyl**= 5-(2,4,6-triisopropylphenyl)-2-(N-2,6-diisopropylphenylformimino)pyrrole; **H_2DPA**= 2,6-pyridine-dicarboxylic acid; **mbpy**= 4,4'-Dimethyl-2,2'-bipyridyl; **btca**= 1,2,4,5-Benzenetetracarboxylic acid; **H_2tbca**= 1,2,4,5-Benzenetetracarboxylic acid; **bpb**= 1,4-bis(pyrid-4-yl)benzene; **TBA**= tetrabutylammonium; **L**^{10*}= N^1,N^2-bis(4-chlorophenyl)oxalamide; **CzPh$_2$PO**= (9H-carbazol-9-yl)diphenylphosphineoxide; **bcpp**= bis(1-chloroimidazo[1,5-*a*]pyridin-3-yl)pyridine; **12-TMC**= 1,4,7,10-tetramethyl-1,4,7,10-tetraazacyclododecane; **dca**= dicyanamide; **atz**= 2-amino-1,3,5-triazine; **L**^{11*}= 4′-(4-methoxyphenyl)-4,2′:6′,4″-terpyridine; **ppad**= N^3-(3-pyridoyl)-3-pyridinecar-boxamidrazone; **dps** = 4,4'-dipyridyl sulfide; **H_3BTB**= 1,3,5-tris(4-carboxylphenyl) benzene; **bim**= 1-benzylimidazole.

Table S2. Coordination networks with dps identified through a systematic search of the Cambridge Structural Database (CSD).

Compound	Formula	Compound type	Methodology	Metal	Year	CCDC	Reference
1	$(C_{20}H_{24}CdN_4O_6S)_n$ $[Cd(CH_3COO)_2(NioxH_2)(dps)]_n$	1D Coordination polymer	The solution was boiled, then cooled to room temperature.	Cd(II)	2012	ZASXEY	54
2	$(C_{18}H_{20}CdN_4O_6S)_n$ $[Cd(CHOO)_2(NioxH_2)(dps)]_n$	1D Coordination polymer	The solution was boiled, then cooled to room temperature	Cd(II)	2012	ZASXIC	54
3	$(C_{20}H_{24}N_4O_6SZn)_n$ $[Zn(CH_3COO)_2(NioxH_2)(dps)]_n$	1D Coordination polymer	The solution was boiled, then cooled to room temperature	Zn(II)	2012	ZASXOI	54
4	$(C_{20}H_{20}CuN_4O_2S_2^{+2})n\cdot 2n(NO_3^-)\cdot 2n(H_2O)$ $\{[Cu(\mu\text{-}dps)_2(H_2O)_2](NO_3)_2\cdot 2H_2O\}_n$	3D Coordination polymer	Stirred / Hydro(solvo)thermal / Filtered/Slow evaporation	Cu(II)	2012	NIMZIT01	55
5	$(C_{20}H_{20}CoN_4O_2S_2^{+2})_n\cdot 2n(C_{10}H_8N_2S)\cdot 2n(NO_3^-)\cdot 4n(H_2O)$ $\{[Co(\mu\text{-}dps)_2(H_2O)_2](NO_3)_2\cdot 2(4,4'\text{-}dps)\cdot 4H_2O\}_n$	3D Coordination polymer	Stirred / Hydro(solvo)thermal / Filtered / Slow evaporation	Co(II)	2012	QEDZIK	55
6	$C_{20}H_{24}CdN_4O_4S_2^{+2}\cdot 2(C_6H_6N_5O^{-2})$	1D Polymeric superstructure	Stirred / Slow evaporation	Cd(II)	2012	LEZBID	56

	$[Cd(H_2O)_4(dps)_2](dmax)_2$						
7	$C_{20}H_{24}N_4O_4S_2Zn^{+2}\cdot 2(C_6H_6N_5O^{-2})$	1D Polymeric superstructure	Stirred / Slow evaporation	Zn(II)	2012	LEZBOJ	56
	$[Zn(H_2O)_4(dps)_2](dmax)_2$						
8	$(C_{40}H_{36}N_4Ni_2O_{10}S_2)_n$	3D Coordination polymer	Hydro(solvo)thermal	Ni(II)	2012	FATBIN	57
	$Ni_2(H_2O)_2(C_{10}H_8O_4)_2(dps)_2$						
9	$C_{27}H_{30}CuN_4O_{11}S_3$	1D Coordination polymer	Stirring / Hydrothermal	Cu(II)	2012	TEBBAF	58
	$\{[Cu(dps)_2(Hssa)(H_2O)_2]\cdot 3H_2O\}_n$						
10	$C_{27}H_{25}MnN_4O_{10}S_3$	1D Coordination polymer	Stirring / Hydrothermal	Mn(II)	2012	TEBBEJ	58
	$\{[Mn(dps)_2(Hssa)(H_2O)_2]\cdot 3H_2O\}_n$						
11	$(C1_8H_{11}BrCoN_2O_4S)_n\cdot 0.5n(C_{10}H_8N_2S_3)$	3D Coordination polymer	Hydrothermal	Co(II)	2013	PEYWAT	59
	$\{[Co(5\text{-}Br\text{-}ip)(dps)](dpts)_{0.5}\}_{2n}$						
12	$(C_{19}H_{14}N_2O_4SZn)_n$	3D Coordination polymer	Hydrothermal	Zn(II)	2013	NIGGOB	60
	$[Zn(mip)(dps)]_n$						
13	$(C_{18}H_{11}BrCoN_2O_4S)_n$	2D Coordination polymer	Hydrothermal	Co(II)	2013	KEYDUP	61
	$[Co(dps)(Brip)]_n$						

14	$(C_{36}H_{24}Br_2N_4Ni_2O_9S_2)_n$ $[Ni_2(H_2O)(5\text{-Br-ip})_2(dps)_2]_n$	3D Coordination polymer	Hydrothermal	Ni(II)	2013	KEYDEZ	62
15	$(C_{52}H_{38}Cu_5N_8O_{30}S_2)_n$ $[Cu_5(nip)_4(\mu_3\text{-}OH)_2(dps)_2(H_2O)_4]_n$	3D Coordination polymer	Hydrothermal	Cu(II)	2013	DINCOU	63
16	$C_{30}H_{20}N_{14}S_{12}Cd_3$ $[H_2(dps)]_2[Cd_3(SCN)_{10}]$	2D Coordination polymer	Slow diffusion	Cd(II)	2013	REQWOB	64
17	$C_{20}H_{18}N_2O_5SCo$ $[Co(Cpp)(dps)(H_2O)]_n$	3D Coordination polymer	Stirring / Hydrothermal	Co (II)	2013	QIXJUE	65
18	$(C_{24}H_{16}CoF_6N_4O_4S_2)_n$ $[Co(tfa)_2(dps)_4]_n$	1D Coordination polymer	Stirred / Precipitate formed on cooling / Filtered	Co(II)	2014	XOGHOS	66
19	$(C_{22}H_{16}CoN_6S_2Se_2)_n\cdot 2n(H_2O)$ $\{[Co(dps)_2(SeCN)_2]\cdot H_2O\}_n$	1D Coordination polymer	Stirred / Slow diffusion	Co(II)	2014	WIZLEY	67
20	$(C_{52}H_{32}Br_4Co_2N_4O_{16}S_2)_n$ $[Co_2(dps)_2(5\text{-Br-Hip})_4]_n$	2D Coordination polymer	Hydrothermal	Co(II)	2014	QIJSIN	68
21	$(C_{70}H_{50}Cd_3N_{28}O_2S_5W_2)_n\cdot 3(H_2O)$ $[Cd(CH_3CN)_2(dps)][Cd(H_2O)(dps)_2]_2[W(CN)_8]_2\cdot 3H_2O$	Sandwich-like coordination network	Slow diffusion	Cd(II), W(IV)	2014	LOMSIR	69

22	$(C_{66}H_{48}Cd_3N_{26}O_4S_5W_2)_n \cdot 2(C_2H_3N) \cdot 4(H_2O)$ $[Cd(H_2O)_2(dps)][Cd(H_2O)(dps)_2]_2[W(CN)_8]_2 \cdot 2CH_3CN \cdot 4H_2O$	Sandwich-like coordination network	Slow diffusion	Cd(II), W(IV)	2014	LOMVEQ	69
23	$(C_{66}H_{48}Cd_3N_{26}O_4S_5W_2)_n \cdot 4(H_2O)$ $[Cd(H_2O)_2(dps)][Cd(H_2O)(dps)_2]_2[W(CN)_8]_2 \cdot 4H_2O$	Sandwich-like coordination network	Slow diffusion	Cd(II), W(IV)	2014	LOMVIU	69
24	$(C_{66}H_{48}Cd_3N_{26}O_4S_5W_2) \cdot 2(C_2H_6O)$ $[Cd(H_2O)_2(dps)][Cd(H_2O)(dps)_2]_2[W(CN)_8]_2 \cdot 2CH_3CH_2OH$	Sandwich-like coordination network	Slow diffusion	Cd(II), W(IV)	2014	LOMVOA	69
25	$(C_{52}H_{56}Cu_4N_4O_{16}S_2)_n \cdot 1.5n(H_2O)$ $[\{Cu_2[CH_3(CH)_2COO]_4(dps)\}_2 \cdot 1.5H_2O]$	1D Coordination polymer	Slow diffusion / Stirred / Filtered / Recrystallized	Cu(II)	2014	KOFZIQ	70
26	$C_{40}H_{36}N_8O_2S_4Zn^{+2} \cdot 2(ClO_4^-) \cdot H_2O$ $Zn(NCO)_2(dps)$	Metal-organic framework	Stirred / Filtered/ Slow evaporation	Zn(II)	2014	FIFZAW01	71
27	$C_{42}H_{32}MnN_{10}S_6$ $Mn(NCS)_2(dps)_4$	Metal-organic framework	Stirred / Slow evaporation	Mn(II)	2014	HOTMIN01	71
28	$(C_{22}H_{16}FeN_6S_4)_n \cdot 2(H_2O)$	Metal-organic framework	Stirred / Filtered	Fe(II)	2014	IREBEN01	71

	$[Fe(NCS)_2(dps)_2]\cdot 2H_2O$						
29	$(C_{12}H_8N_4O_2SZn)_n$ $[Zn(dps)_4(H_2O)_2](ClO_4)2\cdot H_2O$	Metal-organic framework	Refluxed / Filtered / Slow evaporation	Zn(II)	2014	LOHROR	71
30	$(C_{48}H_{32}Cu_8N_{16}S_4)_n$ $[Cu_4(CN)_4(dps)_2]_n$	3D Coordination polymer	Solvothermal	Cu(I)	2014	EFUBAK	72
31	$(C_{46}H_{38}Cu_2I_2N_2P_2S)_n$ 1D-$Cu_2I_2(tpp)_2(dps)$	1D Coordination polymer	Stirred	Cu(I)	2015	SUQFOB	73
32	$(C_{32}H_{24}N_4O_8S_2Zn_2)_n$ [Zn(muco)(dps)]	3D Metal-organic framework	Stirred / Filtered / Slow evaporation	Zn(II)	2015	JUFLED	74
33	$(C_{38}H_{28}Co_2N_4O_{10}S_2)_n$ $[Co_2(dps)_2(CH_3O\text{-}ip)_2]_n$	2D Coordination polymer	Hydro(solvo)thermal	Co(II)	2015	HOMGUN	75
34	$(C_{24}H_{16}N_2NiO_4S)_n$ $[Ni(Bpdc](dps)]_n$	3D Coordination polymer	Hydrothermal	Ni(II)	2015	BOSJAW	76
35	$(C_{48}H_{32}Co_2N_4O_8S_2)_n$ $[Co_2(Bpdc)_2(dps)_2]_n$	3D Coordination polymer	Hydrothermal	Co(II)	2015	FACQOS	76
36	$(C_{29}H_{20}Co_3N_2O_{12}S)_n\cdot 4n(H_2O)$ $[Co_3(\mu_3\text{-}OH)(bppc)(dps)(CH_3CH_2OH)]\cdot 4H_2O$	Coordination polymer	Hydro(solvo)thermal	Co(II)	2015	AHOBAC	77

37	$(C_{56}H_{58}Cu_2N_4O_{11}S_2)_n \cdot H_2O$ $[Cu_2(O_2CC_8H_9)_4(dps)]_n$	Coordination polymer	Slow diffusion / Filtered	Cu(II)	2016	DUYWEB	78
38	$(C_{46}H_{44}Cu_2N_2O_8S)_n$ $[Cu(O_2CC_8H_9)_2(dps)(H_2O)] \cdot H_2O\}_n$	Coordination polymer	Slow diffusion / Filtered	Cu(II)	2016	DUYYON	78
39	$(C_{20}H_{16}F_6N_4S_2SiZn)_n$ $([Zn(dps)_2(SiF_6)] \cdot 4H_2O)$	Metal-organic framework	Slow evaporation	Zn(II)	2017	SAXPIT	79
40	$C_{22}H_{24}CuN_2O_6S$ $\{[Cu(ppa)(dps)(H_2O)](H_2O)_2\}_n$	3D Metal-organic framework	Slow diffusion	Cu(II)	2018	MEFSEY	80
41	$C_{22}H_{22}CuN_2O_5S$ $\{[Cu(ppa)(dps)](H_2O)\}_n$	3D Metal-organic framework	Slow diffusion / Heat	Cu(II)	2018	MEGGEN	80
42	$C_{74}H_{46}Cd_{2.25}Co_{0.75}N_4O_{12}S_2$ $[Cd_{2.25}Co_{0.75}(BTB)_2(dps)_2] \cdot xSol$	2D Metal-organic framework	Single crystal to single crystal conversion	Cd(II), Co(II)	2018	KINSAE	81
43	$C_{24}H_{28}N_4O_{10}S_4Cl_2Cu$ $[Cu(dps)_2(dmso)_2]_n(ClO_4)_{2n}$	2D Coordination polymer	Slow diffusion	Cu(II)	2019	FODDIO02	82
44	$C_{48}H_{60}N_8O_{22}S_8Cl_4Cu_2$ $[\{Cu(dps)_2(dmso)_2\}\{Cu(dps)_2(dmso)(H_2O)\}]_n(ClO_4)_{4n} \cdot 2nH_2O \cdot n(dmso)$	2D Coordination polymer	Slow diffusion	Cu(II)	2019	YONTON	82

45	$C_{40}H_{38}N_8O_{11}S_4Cl_2Co$ $[Co(dps)_4(H_2O)_2](ClO_4)_2]\cdot H_2O$	Coordination complex	Stirred / Slow evaporation	Co(II)	2019	YONTUT	82
46	$(C_{20}H_{16}Br_2CoN_4S_2)_n$ $[Co(dps)_2Br_2]_n$	2D Coordination polymer	Stirred / Filtered / Slow evaporation	Co(II)	2019	POGNAD	30
47	$(C_{20}H_{20}CoN_4O_2S_2^{+2})_n\cdot 4(H_2O)\cdot 2(I^-)$ $[Co(dps)_2(H_2O)_2\cdot I_2\cdot (H_2O)_4]_n$	2D Coordination polymer	Stirred / Filtered / Slow evaporation	Co(II)	2019	POGNEH	30
48	$(C_{24}H_{28}CuN_4O_2S_4^{+2})_n\cdot 2(ClO_4^-)$ $\{[Cu(dps)_2(DMSO)_2](ClO_4)_2\}_n$	2D Coordination polymer	Refluxed / Filtered / Recrystallized	Cu(II)	2019	FODDIO	83
49	$(C_{74}H_{46}Cd_3N_4O_{12}S_2)_n$ $[Cd_3(BTB)_2(dps)_2]\cdot x$Sol	2D Metal-organic framework	Single crystal to single crystal conversion	Cd(II)	2019	FIWGEA	84
50	$(C_{20}H_{16}CuF_6N_4S_2Si)_n\cdot 4(H_2O)\cdot C_2H_2$ $[Cu(dps)_2(SiF_6)]\cdot 6H_2O$	Metal-organic framework	Slow diffusion	Cu(II)	2020	MUBQAE	85
51	$(C_{20}H_{16}CuF_6N_4S_2Si)_n\cdot 4(H_2O)\cdot C_2H_2$ $[Cu(dps)_2(SiF_6)]\cdot 6H_2O$	Metal-organic framework	Slow diffusion	Cu(II)	2020	MUBQAE01	85
52	$(C_{20}H_{16}CuF_6N_4S_2Si)_n\cdot 6(H_2O)$ $[Cu(dps)_2(SiF_6)]$	Metal-organic framework	Slow diffusion	Cu(II)	2020	RUJDIM	85

53	$(C_{34}H_{20}Co_2N_2O_{13}SV)_n$ $[(Co)_2(V)(OH)(NH_2BDC)_3]dps$	Metal-organic framework	Solvothermal	Co(II), V(III)	2020	YUWXUM	86
54	$(C_{16}H_{10}N_2O_4S_2Zn)_n$ [Zn(TDA)(dps)]	2D Metal-organic framework	Hydrothermal	Zn(II)	2020	RUCWAQ	87
55	$C_{36}H_{34}N_6Ni_2O_{12}S_2$	Metal-organic complex	Hydrothermal	Ni(II)	2020	ROXRAA	88
56	$(C_{20}H_{16}CuF_5N_4NbOS_2)_n$ $[Cu(dps)_2(NbOF_5)]$	3D Metal-organic framework	Slow diffusion	Nb(V), Cu(II)	2020	QALNUQ	89
57	$(C_{46}H_{46}Co_3N_2O_{16}S)_n$ $[Co_3(iBuOIPA)_3(dps)(H_2O)]_n$	3D Coordination polymer	Hydrothermal	Co(II)	2020	NUWFIX	90
58	$(C_{32}H_{28}Co_2N_2O_{10}S)_n$ $[Co_2(iPrIPA)_2(dps)]_n$	2D Coordination polymer	Hydrothermal	Co(II)	2020	NUWFOD	90
59	$(C_{20}H_{16}CuF_6GeN_4S_2)_n$ $[Cu(dps)_2(GeF_6)]$	Metal-organic framework	Slow diffusion / Filtered	Cu(II), Ge(IV)	2020	NUQGEO	91
60	$(C_{20}H_{16}F_6GeN_4S_2Zn)_n$ $[Zn(dps)_2(GeF_6)]$	Metal-organic framework	Slow diffusion / Filtered	Ge(IV), Zn(II)	2020	NUQGUE	91
61	$(C_{50}H_{46}Cu_2N_6O_{18}S_2)_n \cdot 12(H_2O)$ $\{[Cu(Cbdcp)(dps)(H_2O)_3]\cdot 6H_2O\}_n$	1D Metal-organic framework	Stirred / Crystallized / Filtered	Cu(II)	2020	IQIVAI	92

62	$(C_{96}H_{72}Cu_4N_{12}O_{18}S_2)_n$ $[Cu_4(Dcbb)_4(dps)_2(H_2O)_2]_n$	1D Metal-organic framework	Stirred / Crystallized / Filtered	Cu(II)	2020	IQIVEM	92
63	$(C_{20}H_{16}CuF_6GeN_4S_2)_n \cdot 6(H_2O)$ $[Cu(dps)_2(GeF_6)]_n$	Metal-organic framework	Slow diffusion / Filtered	Cu(II), Ge(IV)	2022	FAWXOU	93
64	$(C_{20}H_{16}CuF_5N_4NbOS_2)_n \cdot 8(H_2O)$ $[Cu(dps)_2(NbOF_5)]_n$	Metal-organic framework	Slow diffusion / Filtered	Cu(II), Nb(V)	2022	FAWXUA	93
65	$C_{20}H_{16}Cl_2CoN_4S_2$ $[Co(dps)_2Cl_2]_n$	2D Metal-organic framework	Stirred / Heated / Slowly evaporated	Co(II)	2023	PUQGAJ02	94
66	$C_{34}H_{24}Mg_2N_2O_{10}S$ $[Mg_2(1,4\text{-}NDC)_2(H_2O)_2] \cdot [(dps)_2]$	3D Metal-organic framework	Stirred / Heated / Slowly evaporated	Mg(II)	2023	UDUSAR	95

$NioxH_2$= 1,2-cyclohexanedionedioxime; **dmax**= 4,6-dimethyl-1,2,3-triazolo[4,5-d]pyrimidin-5,7-dionato; **Hssa**= 5-sulfosalicylic acid; **dpts**= dipyridyltrisulfide; **mip**= 5-methylisophthalic acid; **Brip**= 4-bromoisophthalate; **5-Br-ip**= 5-bromoisophthalate; **nip**= 5-nitroisophthalic acid; **Cpp**= 3(4carboxyphenyl)propionic acid; **tfa**$^-$= $CF_3CO_2^-$; **5-Br-Hip**= 5-bromoisophthalate; **tpp**= triphenylphosphine; **muco**= trans-muconate dianion; **CH_3O-H_2ip**= 5-methoxyisophthalate; **Bpdc**= 3,3'-biphenyl dicarboxylic; **bppc**= biphenyl-2,4,6,3',5'-pentacarboxylic**;** **ppa**= 1,4-phenylenedipropionic acid; **BTB**= benzene-1,3,5-tribenzoic acid; **NH_2BDC**= 2-amino-benzene-1,4-dicarboxylate; **TDA**= 2,5-thiophene dicarboxylic acid; **iBuOIPA**= 5-i-butoxyisophthalate; **iPrIPA**= 5-i-propoxyisophthalate; **Cbdcp**= N-(4-carboxybenzil)-(3,5-dicarboxyl)-pyridinium; **Dcbb**= 1-(3,5-dicarboxybenzyl)-4,4'-bipyridinium; **1,4-NDC**= 1,4-naphthalenedicarboxylic acid.

Table S3. A set of abbreviations used to designate 4,4’-dipyridyl sulfide (dps) through a systematic search of the Cambridge Structural Database (CSD).

Abbreviations	Nomenclature	Number of reports	References
Bds	4,4'-bipyridyl sulfide	1	65
bps	4,4'-bipyridylsulfide	1	67
bps	4,4'-bipyridyl sulfide	2	90
bps	4,4'-bipyridyl sulphide	2	56
dbs	4,4'-dipyridylsulfide	2	74, 89
dps	4,4’-dipyridylsulfide	23	54, 58-60, 62, 63, 68, 72, 75, 79, 85, 86, 88, 93
dps	4,4’-dipyridyl sulfide	11	66, 69, 1, 83, 84, 92
dps	di(4-pyridyl)sulfide	6	78, 81, 82
dps	dipyridin-4-ylsulfane	1	94
dps	4,4′-dipyridinesulfide	1	87
dps	4,4'-sulfanediyldipyridine	1	77
Dps	4,4'-dipyridyl sulfide	2	76
DPS	di(4-pyridyl)sulphide	4	71
S-(Py)2	di(4 pyridinyl) sulfide	1	95
tdp	4,4’-thiodipyridine	2	80
tdpy	4,4’-thiodipyridine	1	64
	4,4'-thiodipyridine	1	57
4-dps	4,4'-dipyridyl sulfide	1	70
4,4'-dps	4,4′-Dipyridylsulfide	1	73
4,4'-dps	di(4-pyridyl)sulfide	2	55

Table S4. Coordination networks with dpds identified through a systematic search of the Cambridge Structural Database (CSD).

Compound	Formula	Compound type	Methodology	Metal	Year	CCDC	Reference
1	$C_{30}H_{28}N_6O_8S_6Cu$ $[Cu(dpds)_2(H_2O)_2](3pySO_3)_2$	1D Coordination polymer	Slow diffusion	Cu(II)	2012	RAFVIF	96
2	$C_{30}H_{32}S_6O_{10}N_6Zn$ $[Zn(dpds)_2(H_2O)_2](3pySO_3)_2 \cdot 2H_2O$	1D Coordination polymer	Stirring	Zn(II)	2012	RAFVOL	96
3	$C_{28}H_{34}S_4O_{14}N_4Zn$ $[Cu(dpds)_2(H_2O)_2](Hfum)_2 \cdot 4H_2O$	1D Coordination polymer	Reflux/ filtration	Cu(II)	2012	RAFVUR	96
4	$C_{28}H_{36}S_4O_{15}N_4Zn$ $[Zn(dpds)_2(H_2O)_2](Hfum)_2 \cdot 5H_2O$	1D Coordination polymer	Hydro(solvo) thermal	Zn(II)	2012	RAFWAY	96
5	$C_{41}H_{36}MnN_4O_8S_4$ $[\{Mn(O_2CPh)_2(dpds)_2\} \cdot (H_2O) \cdot 0.5(HO_2CPh)]_n$	1D Coordination polymer	Slow diffusion	Mn (II)	2012	GEBZAQ	97
6	$Mn_2C_{54}H_{40}N_{14}S_{14}O$ $[Mn(NCS)_2(dpds)_2]_2 \cdot DPDS \cdot H_2O$	1D Coordination polymer	Reaction mixture/crystallization	Mn(II)	2012	CEWFOB	98

7	$FeC_{22}H_{22}N_6O_3S_6$ $[Fe(NCS)_2(dpds)_2]\cdot 3H_2O$	1D Coordination polymer	Slow diffusion	Fe(II)	2012	CEWFUH	98
8	$CoC_{22}H_20N_6O_2S_6$ $[Co(NCS)_2(dpds)_2]\cdot 2H_2O$	1D Coordination polymer	Slow diffusion	Co(II)	2012	CEWGAO	98
9	$C_{26}H_{24}N_4O_{10}S_4Zn_2$ $Zn_2(dpds)_2(C_3H_2O_4)_2(H_2O)_2$	2D Coordination polymer	Stirring under heat/ crystallization	Zn(II)	2012	KESBAN	99
10	$C_{10}H_8Cl_2N_2S_2Zn$ $(C_{10}H_8Cl_2N_2S_2Zn)_n$	1D Coordination polymer	Slow diffusion	Zn(II)	2012	YEJDAU	100
11	$C_{10}H_8Br_2N_2S_2Zn$ $[ZnBr_2(\mu\text{-dpds})]_n$	1D Coordination polymer	Slow evaporation	Zn(II)	2013	REPTEN	101
12	$C_{44}H_{38}N_{12}O_7S_8Co_2$ $[Co_2(NCO)_4(dpds)_4]\cdot 3H_2O$	3D Coordination polymer	Slow evaporation	Co(II)	2013	GIDWEX	102
13	$C_{15}H_{19}N_2O_9S_2Zn$ $\{[Zn(C_{10}H_2O_8)_{0.5}(dpds)]\cdot 5H_2O]\}_n$	2D Metal-organic framework	Slow diffusion	Zn(II)	2013	PITRIV	103
14	$C_{12}H_{20}N_2S_2O_{10}Cu$ $[Cu(C_2O_{4)}(dpds)]\cdot 6H_2O$	2D Coordination polymer	Hydrothermal	Cu(II)	2013	DIMPUM	104
15	$C_{22}H_{22}N_4S_4O_7Cu$	1D Coordination polymer	Stirring/ reflux/ filtration	Cu(II)	2013	DIMYUV	104

	$[Cu(C_2O_4)(dpds)_2]\cdot 3H_2O$						
16	$(C_{36}H_{26}Co_2N_6O_{14}S_4)_n$ $[Co(H_2O)(dpds)(nip)]_n$	3D Coordination polymer	Hydrothermal	Co(II)	2013	KEYDOJ	61
17	$C_{26}H_{28}Cu_2N_2O_8S_2$ $[Cu_2[CH_3(CH)_2COO]_4(dpds)]$	1D Coordination polymer	Slow diffusion	Cu(II)	2014	KOFZEM	70
18	$(C_{30}H_{22}Co_2N_4O_{12}S_4)$ $[Co(dpds)(pyromellitate)_{0.5}(H_2O)_2]_n$	2D Metal-organic framework	Slow diffusion	Co(II)	2014	LOCZAG	105
19	$(C_{30}H_{24}CuN_4O_{10}S_4)$ $[Cu(dpds)_2(pyromellitate)]_n\cdot 2_n(H_2O)$	2D Metal-organic framework	Slow diffusion	Cu(II)	2014	LOCZEK	105
20	$(C_{34}H_{60}N_4Ni_2O_{25}S_4)$ $[Ni_2(dpds)_2(pyromellitate)(H_2O)_2]_n\cdot 2n(C_2H_5OH)\cdot 11n(H_2O)$	3D Metal-organic framework	Slow diffusion	Ni(II)	2014	LOCZIO	105
21	$C_{16}H_{17}N_2O_5S_2Cu$ $Cu(H_2O)(dpds)(2\text{-}MGA)$	2D Coordination polymer	Slow evaporation	Cu(II)	2014	AJULIC	106
22	$C_{16}H_{18.5}N_2O_{5.25}S_2Zn$ $Cu(H_2O)(dpds)(2\text{-}MGA)$	3D Coordination polymer	Hydrothermal	Zn(II)	2014	AJULEY	106

23	$C_{16}H_{16.5}N_2O_{5.25}S_2Cd$ $[Cd(H_2O)(dpds)(2\text{-}MGA)]\cdot 0.25H_2O$	3D Coordination polymer	Slow evaporation	Cd(II)	2014	AJULAU	106
24	$C_{26}H_{19}N_8S_6FeCl$ $\{[Fe(NCS)_2(dpds)_2]\cdot 2(2,5\text{-}DCP)\}_n$	3D Coordination polymer	Stirring/ slow evaporation	Fe(II)	2015	GOTZEW	107
25	$C_{26}H_{24}N_4O_6S_4Zn$ $[Zn(muco)(dpds)_2(H_2O)_2]$	2D Supramolecular network	Stirring/ slow evaporation	Zn(II)	2015	JUFZAN	74
26	$C_{44}H_{40}N_4O_{14}S_4Zn_2$ $\{[Zn(2,6\text{-}ndc)(dpds)]\cdot 3(H_2O)\}_n$	2D Metal-organic framework	Slow diffusion	Zn(II)	2015	WUGZUV	108
27	$C_{22}H_{22}CoN_2O_8S_2$ $\{[Co(2,6\text{-}ndc)(dpds)(H_2O)_2]\cdot 2(H_2O)\}_n$	2D Metal-organic framework	Slow diffusion	Co(II)	2015	WUHBAE	108
28	$C_{56}H_{52}Cd_2N_6O_{14}S_6$ $\{[Cd_2(2,6\text{-}ndc)_2(dpds)_2(H_2O)_2]\cdot (dpds)\cdot(EtOH)\cdot 3(H_2O)\}_n$	3D Metal-organic framework	Slow diffusion	Cd(II)	2015	WUJRUQ	108
29	$C_{37.24}H_{36.96}N_4O_{17.24}S_4Zn_2$ $\{[Zn(bdc)(dpds)]\cdot 0.62(MeOH)\cdot 2(H_2O)\}_n$	2D Metal-organic framework	Direct mixing	Zn(II)	2015	GOVYOH	109

30	$C_{15}H_{19}N_2O_{14}S_2Zn$ $\{[Zn(C_{10}H_2O_8)_{0.5}(dpds)]\cdot 5H_2O]\}_n$	2D Metal-organic framework	Slow diffusion	Zn(II)	2015	PITRIV01	110
31	$C_{34}H_{46}Cu_2N_6O_{20}S_4$ $[Cu_2(PDA)_2(dpds)_2(H_2O)_2].8H_2O$	Dimeric structure linked through H-bonding to form 1D chain.	Slow diffusion	Cu(II)	2016	AKIPER	111
32	$C_{36}H_{26}Cu_2N_4O_4S_2$ $[Cu(L)]_2(dpds)]_n$	3D Coordination polymer	Stirring/recrystallization	Cu(II)	2017	XESWUQ	112
33	$C_{10}H_8Cl_2HgN_2S_2$ $[Hg(dpds)Cl_2]_n$	1D Coordination polymer	Slow diffusion	Hg(II)	2017	NATGIB	113
34	$C_{10}H_8Br_2HgN_2S_2$ $[Hg(dpds)Br_2]_n$	1D Coordination polymer	Slow diffusion	Hg(II)	2017	NATGOH	113
35	$C_{10}H_8I_2HgN_2S_2$ $[Hg(dpds)I_2]_n$	1D Coordination polymer	Slow diffusion	Hg(II)	2017	NATKEB	113
36	$C_{25}H_{28}Cu_2N_4O_{14}S_2$ $\{[Cu_2(2,5\text{-}pdc)_2(dpds)(H_2O)_2]\cdot 3H_2O\cdot MeOH\}_n$	3D Metal-organic framework	Slow diffusion	Cu(II)	2018	IMOTAG02	114
37	$C_{74}H_{46}Cd_3N_4O_{12}S_4$ $[Cd_{2.2}5Co_{0.75}(BTB)_2(dpds)_2]\cdot xSol$	2D Metal-organic framework	Single-crystal to single-crystal conversion	Cd(II), Co(II)	2018	KINSEI	81

38	$C_{48}H_{74}Cu_2N_7O_{13.5}S_2$ $[Cu_2(caproxy)_4(dpds)]_n$	1D Coordination polymer	Single-crystal to single-crystal conversion	Cu(II)	2018	ONODED	115
39	$C_{38}H_{24}FeN_{12}S_6$ $[Fe(dpds)_2\{C(CN)_3\}_2]\cdot dpds$	1D Coordination polymer	Stirring/crystallization	Fe(II)	2019	XOHKOX	116
40	$C_{22}H_{22}B_2FeN_6S_4$ $[Fe(dpds)_2(NCBH_3)_2]$	1D Coordination polymer	Slow diffusion	Fe(II)	2019	XOHLAK	116
41	$C_{22}H_{23}FeN_6S_4O_{3.5}Se_2$ $[Fe(dpds)_2(NCSe)_2]\cdot 3.5H_2O$	1D Coordination polymer	Slow diffusion	Fe(II)	2019	XOHLIS	116
42	$C_{28}H_{24}CoN_4O_6S_4$ $[Co(dpds)(bdc)(H_2O)_2].dpds$	2D Metal-organic compound	Slow diffusion	Co(II)	2020	NUJFAC	117
43	$C_{28}H_{24}CuN_4O_6S_4$ $[Cu(dpds)(bdc)(H_2O)_2]$	2D Coordination polymer	Slow evaporation	Cu(II)	2020	ELUWEQ	118
44	$C_{48}H_{41}Mn_2N_{16}NbO_{4.5}S_8$ $[Mn(dpds)_2]_2[Nb(CN)_8]\cdot 6H_2O$	3D Coordination framework	Slow diffusion	Mn(II)	2021	PARLON	119
45	$C_{18}H_{15}N_3O_5S_2Zn$ $[Zn(5\text{-}AIP)(dpds)]\cdot H_2O$	2D Coordination polymer	Slow diffusion	Zn(II)	2021	ITESUY	120
46	$C_{40}H_{32}Mo_2N_8Ni_2O_8S_8$ $[Ni(dpds)]_2MoO_4$	2D Pillared rhomboid grids	Stirring/ filtration	Ni(II), Mo(VI)	2022	YAPBAW	121

47	$C_{40}H_{32}N_8Ni_2O_8S_8W_2$ $[Ni(dpds)]_2WO_4$	2D Pillared rhomboid grids	Stirring/ filtration	Ni(II), W(VI)	2022	YAPBEA	121
48	$C_{40}H_{32}Cr_2N_8Ni_2O_8S_8$ $[Ni(dpds)]_2CrO_4$	2D Pillared rhomboid grids	Stirring/ filtration	Ni(II), Cr(VI)	2022	YAPCEB	121
49	$C_{20}H_{16}CuN_4S_4 \cdot 2(BF_4)$ $(Cu(BF_4)_2(dpds)_2)$	1D Metal-organic framework	Stirring/crystallization	Cu(II)	2024	QOGTUF	122
50	$C_{30}H_{30}Cu_2N_4O_{17}S_4$ $[Cu_2(dpds)_2(C_5O_5)_2(H_2O)_4] \cdot 3H_2O$	1D Coordination polymer	Reaction mixture/ crystallization	Cu(II)	2024	COZRAO	123
51	$C_{15}H_{14}CuN_2O_8S_2$ $[Cu(dpds)(C_5O_5)] \cdot 3H_2O$	2D Metal-organic framework	Reaction mixture/crystallization	Cu(II)	2024	COZRES	123
52	$C_{32}H_{40}Cu_2N_4O_{20}S_4$ $[Cu_2(dpds)_2(C_5O_5)_2] \cdot 9H_2O \cdot C_2H_5OH$	3D Metal-organic framework	Reaction mixture/crystallization	Cu(II)	2024	COZRIW	123

3pySO$_3$H= pyridine-3-sulfonic acid; **H$_2$fum**= fumaric acid; **H$_2$nip**= 5-nitroisophthalic acid; **H$_2$MGA**= (RS)-2-methyl glutaric acid; **2,5-DCP**= 2,5-dichloropyrazine; **muco**= trans-muconate; **2,6-ndc**= 2,6-naphthalene dicarboxylic acid; **bdc**= benzenedicarboxylic acid; **PDA**= 2,4-pyridine; **H$_2$L**= salicylidene-2-aminopheno; **2,5-pdc**= 2,5-pyridine-dicarboxylate; **BTB**= benzene-1,3,5-tribenzolate; **Hcaproxy**= 3-carboxy-2,2,5,5-tetramethyl1-pyrrolidinyloxy; **5-AIP** =5-amino isophthalate.

Table S5. A set of abbreviations used to designate 4,4'-dipyridyl disulfide (dpds) through a systematic search of the Cambridge Structural Database (CSD).

Abbreviations	Nomenclature	Number of reports	References
Ald	aldrithiol	1	111
ald-4	aldrithiol-4	1	114
Ald-4	aldrithiol-4	1	120
	aldrithiol	2	103, 110
aldrithiol	4,4′-dipyridyldisulfide	3	105
aldrithiol	4,4′-dipyridyl disulphide	3	108
bpds	4,4′-bipyridyldisulphid	1	117
bpds	4,4′-dipyridyldisulfide	1	99
bpds	bis(4-pyridyl)disulfide	3	113
dbds	4,4'-dipyridyldisulfide	1	74
dpds	4,4'-bipyridinedisulfide	1	122
dpds	4,4'-dipyridyldisulfide	13	61, 96, 109, 116, 119, 123
Dpds	4,4′-dipyridyldisulfide	3	106
DPDS	4,4′-bipyridinedisulfide	3	121
DPDS	4,4'-dipyridyl disulfide	1	81
DPDS	di(4-pyridyl)disulfide	4	98, 102
dtdp	4,4'-dithiodipyridine	2	100, 101
pds	4,4'-dipyridyl disulfide	1	115
SS	4,4′-dipyridyldisulfide	2	104
4,4′-dtp	4,4′-dithiopdipyridine	1	97
4,4'-dtdp	4,4′-dithiodipyridine	1	112
4-dpds	4,4'-dipyridyldusulfide	1	118
4-dpds	4,4'-dipyridyl disulfide	1	70
4-DPS	4,4'-dipyridyl disulfide	1	107

Table S6. Selected bond distances for compounds **1-2.**

Atom labels	1 (M= Co)	2 (M=Cu)
M1—O1	2.218(4)	2.034(3)
M1—O2	2.049(3)	1.989(3)
M1—N3	2.100(5)	1.997(3)
M1—O5^{i}	2.048(3)	1.977(3)
M1—O6^{i}	2.194(5)	2.499(3)
M1—N4^{ii}	2.123(5)	2.263(3)
C1—C2	1.536(8)	1.541(6)
C9—C10	1.553(8)	1.550(5)
S1—C15	1.776(7)	1.771(4)
S1—C16	1.776(7)	1.781(5)
N1—C1	1.339(7)	1.318(6)
N1—C3	1.412(8)	1.422(5)
N2—C7	1.418(7)	1.416(6)
N2—C9	1.333(8)	1.333(5)
C15—S1—C16	101.1(3)	101.2(2)
C1—N1—C3	127.6(5)	127.0(4)
C7—N2—C9	126.2(5)	125.8(4)

Table S7. Geometric analysis of the coordination environment of the Co^{II} **(1)** and Cu^{II} **(2)** ions, showing the site symmetry approximation derived from continuous shape measures (CShM; via SHAPE[124]).

Label	Symmetry	Shape	CShM*	
			(1)	**(2)**
HP-6	D_{6h}	Hexagon	15.103	15.625
PPY-6	C_{5v}	Pentagonal pyramid	25.462	25.499
JBTPR-8	C_{2v}	Octahedron	16.441	17.359
TPR-6	D_{3h}	Trigonal prism	21.941	23.105
JPPY-6	C_{5v}	Johnson pentagonal pyramid J2	25.329	25.733

*The approach is incorporated into the program SHAPE, which is readily available for public use.[124] The values of SHAPE measures relative to other reference polyhedra of **1** are significantly larger. The lower limit corresponds to structures that exactly match the shape of symmetry, and increasing values result in increasingly distorted structures.[125]

1. *Ab Initio* Energy Levels

The SA-CASSCF(7,5)/SC-NEVPT2 calculations yielded 50 spin-free states. The energies of the lowest 7 states, corresponding to the parent ^{4}F and ^{4}P terms, are provided in Table S8. The subsequent spin-orbit coupling (SOC) calculation generated 120 spin-orbit states.

Table S8. Energies of the lowest spin-free states from NEVPT2 calculation.

State (S = 3/2)	Symmetry	Energy (cm^{-1})
1	^{4}F	0.0
2	^{4}F	343.6
3	^{4}F	1614.1
4	^{4}F	8549.9
5	^{4}P	8750.9
6	^{4}F	8894.6
7	^{4}P	17984.9

Table S9. Energies of the lowest 12 spin-orbit states (Kramers Doublets 1-6).

State	Energy (cm^{-1})
1, 2	0.0
3, 4	228.1
5, 6	651.5
7, 8	926.5
9, 10	1975.2
11, 12	2032.8

2. Ground State Spin Hamiltonian Parameters (Multiplet 1)

The ground S=3/2 pseudospin multiplet (composed of states 1-4) was analyzed. The principal values and orientation vectors for the g-tensor and D-tensor relative to the molecular Cartesian frame are provided in Tables S10 and S11, respectively.

Table S10. Selected bond distances for compounds **1-2.**

Axis	g-value	v_x	v_y	v_z
g_x (Xm)	1.8857	-0.15137	-0.98840	-0.01269
g_y (Ym)	2.1449	0.98848	-0.15134	-0.00348
g_z (Zm)	3.1130	0.00152	-0.01307	0.99991

Table S11. Selected bond distances for compounds **1-2.**

Axis	D-value (cm^{-1})	v_x	v_y	v_z
D_x (Xa)	-70.657	0.00842	-0.01074	0.99991
D_y (Ya)	10.992	0.99936	-0.03470	-0.00879
D_z (Za)	59.665	-0.03479	-0.99934	-0.01044

The *D* and *E* parameters derived from these tensor components are D = -106.0 cm^{-1} and E = -24.3 cm^{-1}.

3. Ground State ZFS Matrix and QTM Analysis

The large rhombicity ($|E/D| \approx 0.23$) induces significant mixing of the M_S states. This is quantified in the *ab initio* ZFS matrix (Table S12), which shows large off-diagonal elements (e.g., 41.0 + 9.8*i* cm^{-1}) coupling the ground and excited doublets.

Table S12. Selected bond distances for compounds **1-2.**

	|-3/2⟩	**|-1/2⟩**	**|+1/2⟩**	**|+3/2⟩**
⟨-3/2|	-105.98	0.69 - 0.89i	41.00 + 9.79i	0.00 - 0.00i
⟨-1/2|	0.69 + 0.89i	105.98	0.00 - 0.00i	41.00 + 9.79i
⟨+1/2|	41.00 - 9.79i	0.00 + 0.00i	105.98	-0.69 + 0.89i
⟨+3/2|	0.00 + 0.00i	41.00 - 9.79i	-0.69 - 0.89i	-105.98

4. Anisotropy of Excited Multiplets

The spin Hamiltonian parameters for all 10 calculated multiplets (9 of S = 3/2, 1 of S = 1/2) are summarized in Table S13.

Table S13. Energies, *g*-tensor values, and ZFS parameters for all calculated multiplets.

Mult.	**Energy Range (cm^{-1})**	**g_x**	**g_y**	**g_z**	**D (cm^{-1})**	**E (cm^{-1})**
1	0 – 228	1.886	2.145	3.113	-106.0	-24.3
2	651 – 926	2.101	1.957	1.094	134.6	-16.2
3	1975 – 2032	1.710	1.825	1.962	27.9	-4.3
4	8861 – 8905	2.124	2.037	1.830	-21.1	-3.7
5	9058 – 9099	1.605	1.864	2.164	19.4	-4.0
6	9250 – 9387	1.441	1.508	1.997	-66.5	-8.9
7	10711 – 12899	0.985	0.985	0.993	1051.2	-175.0
8	18272 – 18312	1.630	1.691	1.801	19.7	-1.9
9	18543 – 18779	0.718	0.896	1.293	111.2	-22.8
10	19080	1.006	1.291	1.780	N/A	N/A

5. Crystal Field Parameters

The *ab initio* crystal field was fitted to the spin-free ^{4}F term (L=3). The resulting Extended Stevens Operator (O_k^q) parameters (B_k^q) are given in Table S14.

Table S14. *Ab initio* crystal field parameters B_k^q (in cm^{-1}) for the L=3 (^{4}F) ground term, using the Extended Stevens Operator definition.

k	q	B_kq (cm^{-1})	k	q	B_kq (cm^{-1})
2	-2	47.500	4	0	-10.668
2	-1	0.310	4	1	45.313
2	0	24.891	4	2	9.100
2	1	-28.088	4	3	40.849
2	2	-39.733	4	4	-12.456
4	-4	72.742	6	-6	0.339
4	-3	86.807	6	-5	0.538
4	-2	-15.727	6	-4	0.159
4	-1	56.165	6	-3	0.307
			6	-2	0.394
			6	-1	-0.282
			6	0	0.024
			6	1	-0.380
			6	2	-0.020
			6	3	0.859
			6	4	0.091
			6	5	1.970
			6	6	0.236

Table S15. Generalized Debye parameters from the ac data measured in absence of a magnetic field for **1**.

T / K	H / Oe	τ / s	χ_S / cm^{3}mol^{-1}	χ_T / cm^{3}mol^{-1}	α
2.59892	0.343	8.33×10^{-5}	0.88099	0.89744	0.09209
2.79978	0.343	8.10×10^{-5}	0.8187	0.83491	0.13221
3.00027	0.343	7.02×10^{-5}	0.76579	0.77838	2.61×10^{-8}
3.19881	0.343	7.05×10^{-5}	0.7187	0.73051	2.26×10^{-5}
3.39925	0.343	6.89×10^{-5}	0.67666	0.68883	0.06975
3.60116	0.343	6.52×10^{-5}	0.63943	0.65064	0.05305
3.79996	0.343	5.12×10^{-5}	0.60275	0.61929	0.37666
3.99919	0.343	6.81×10^{-5}	0.57612	0.58687	0.10576
4.4995	0.343	5.45×10^{-5}	0.51272	0.52104	3.10×10^{-20}
5.50019	0.343	6.19×10^{-5}	0.4203	0.42901	0.25124
5.99961	0.343	5.26×10^{-5}	0.38668	0.39234	1.09×10^{-10}
6.50013	0.343	4.59×10^{-5}	0.35712	0.36183	1.34×10^{-16}

Table S16. Generalized Debye parameters from the ac data measured with an applied field of 1kOe for **1**.

T / K	H / Oe	τ / s	χ_S / cm^{3}mol^{-1}	χ_T / cm^{3}mol^{-1}	α
2.00304	1000.137	3.76×10^{-4}	0.13676	0.99959	0.1341
2.20328	1000.137	3.34×10^{-4}	0.12744	0.94288	0.1189
2.40255	1000.137	2.94×10^{-4}	0.12035	0.88628	0.10141
2.60222	1000.137	2.61×10^{-4}	0.11284	0.8381	0.09235
2.80221	1000.137	2.30×10^{-4}	0.10633	0.79027	0.08267
3.00224	1000.137	2.01×10^{-4}	0.10136	0.74512	0.07209
3.20213	1000.137	1.78×10^{-4}	0.09513	0.70759	0.07076
3.40193	1000.137	1.56×10^{-4}	0.09062	0.67016	0.06446
3.60153	1000.137	1.37×10^{-4}	0.08573	0.63778	0.06305
3.80155	1000.137	1.21×10^{-4}	0.0821	0.60649	0.05862
4.00085	1000.137	1.06×10^{-4}	0.07751	0.57893	0.05882
4.50096	1000.137	7.65×10^{-5}	0.07131	0.51449	0.04573
5.00068	1000.137	5.63×10^{-5}	0.06524	0.46631	0.04207
5.50075	1000.137	4.14×10^{-5}	0.06083	0.42426	0.0366
6.00011	1000.137	3.08×10^{-5}	0.05693	0.38896	0.03133
6.49973	1000.137	2.32×10^{-5}	0.05459	0.35946	0.0269
6.99932	1000.137	1.76×10^{-5}	0.05113	0.3339	0.02442
7.49891	1000.137	1.32×10^{-5}	0.04541	0.31197	0.02931
7.99941	1000.137	1.01×10^{-5}	0.04158	0.29268	0.03328
8.49913	1000.137	7.58×10^{-6}	0.0334	0.27496	0.03425
8.999	1000.137	5.61×10^{-6}	0.02565	0.26031	0.05053
9.49887	1000.137	3.82×10^{-6}	2.03×10^{-12}	0.24667	0.06824

Table S17. Generalized Debye parameters from the ac data measured with an applied field of 1kOe for **2**.

T / K	H / Oe	τ / s	χ_S / cm^{3}mol^{-1}	χ_T / cm^{3}mol^{-1}	α
1.99999	1000.266	1.63×10^{-4}	0.04429	0.08521	0.09875
2.20018	1000.266	2.04×10^{-4}	0.05018	0.09326	0.08176
2.40022	1000.266	2.68×10^{-4}	0.05637	0.10794	0.13947
2.6001	1000.266	3.08×10^{-4}	0.06098	0.11572	0.15829
2.80028	1000.266	3.00×10^{-4}	0.06367	0.11389	0.10773
3.00019	1000.266	3.29×10^{-4}	0.06356	0.11623	0.16315
3.20011	1000.266	3.00×10^{-4}	0.06152	0.11221	0.15091
3.39999	1000.266	2.83×10^{-4}	0.06012	0.10805	0.15715
3.59981	1000.266	2.68×10^{-4}	0.05832	0.10462	0.14349
3.80002	1000.266	2.32×10^{-4}	0.05561	0.10035	0.14133
4.00007	1000.266	2.08×10^{-4}	0.05325	0.09563	0.12881
4.49984	1000.266	1.74×10^{-4}	0.04759	0.08753	0.13278
5.00009	1000.266	1.35×10^{-4}	0.04261	0.07799	0.11149
5.5001	1000.266	1.10×10^{-4}	0.03782	0.07152	0.14518
5.9998	1000.266	8.52×10^{-5}	0.03481	0.06404	0.11137
6.4999	1000.266	7.20×10^{-5}	0.03107	0.06021	0.1516
7.00011	1000.266	5.77×10^{-5}	0.02902	0.05464	0.1236
7.49996	1000.266	4.64×10^{-5}	0.02611	0.05094	0.15513
7.99988	1000.266	4.17×10^{-5}	0.02502	0.0473	0.11817
8.49983	1000.266	2.57×10^{-5}	0.01849	0.04596	0.31435
9.00002	1000.266	2.60×10^{-5}	0.02049	0.0414	0.19429
9.49998	1000.266	2.46×10^{-5}	0.02049	0.03854	0.13666
10.00009	1000.266	1.43×10^{-5}	0.01523	0.03723	0.304
10.50047	1000.266	1.33×10^{-5}	0.01499	0.03461	0.2571
11.50001	1000.266	1.27×10^{-5}	0.01557	0.0308	0.2066

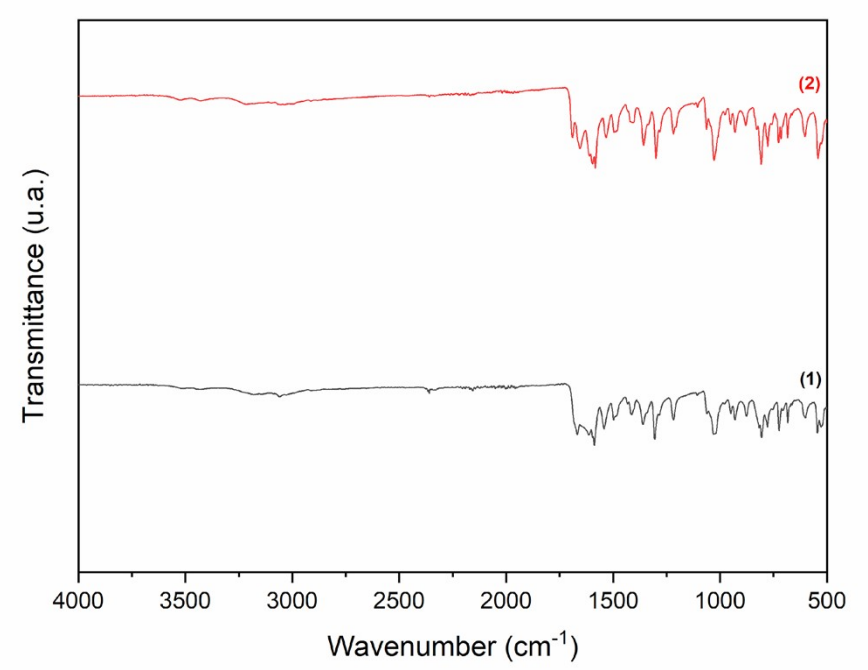

Figure S1. FTIR spectra of **1** (black trace) and **2** (red trace).

(a)

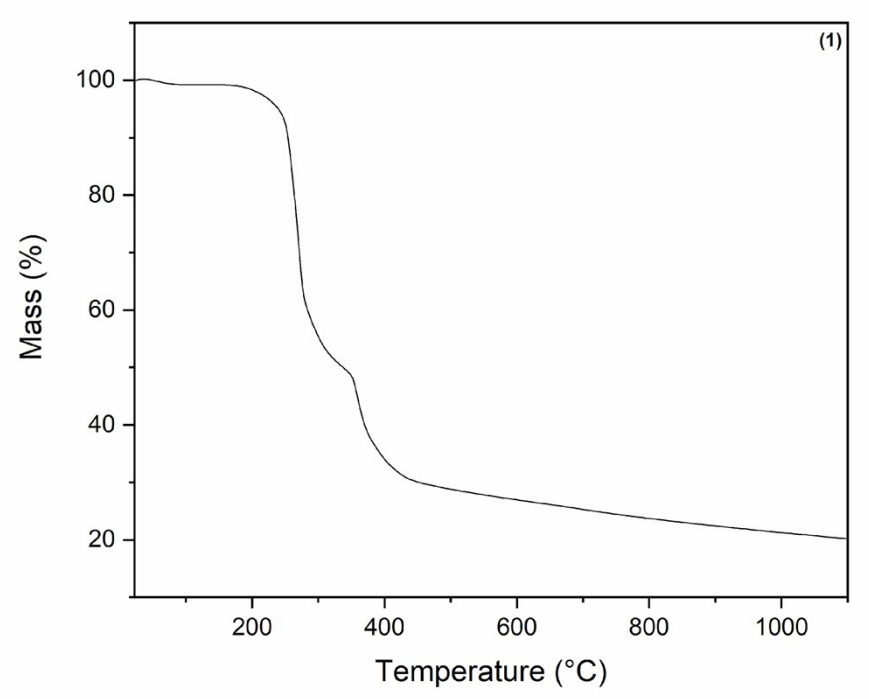

(b)

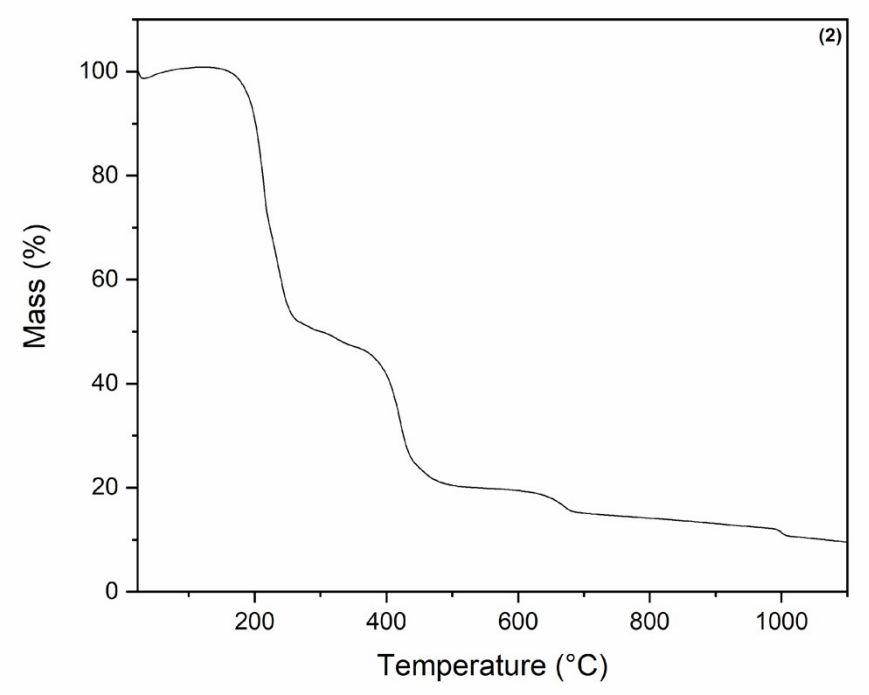

Figure S2. Thermogravimetric curves for **1** (a) and **2** (b).

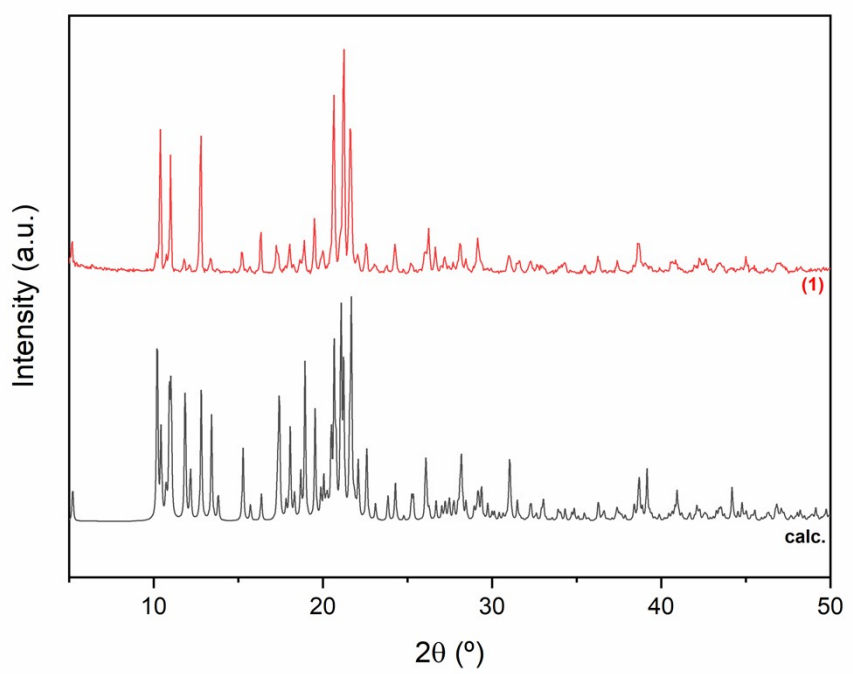

Figure S3. Experimental (red) and calculated (black) PXRD patterns for **1**.

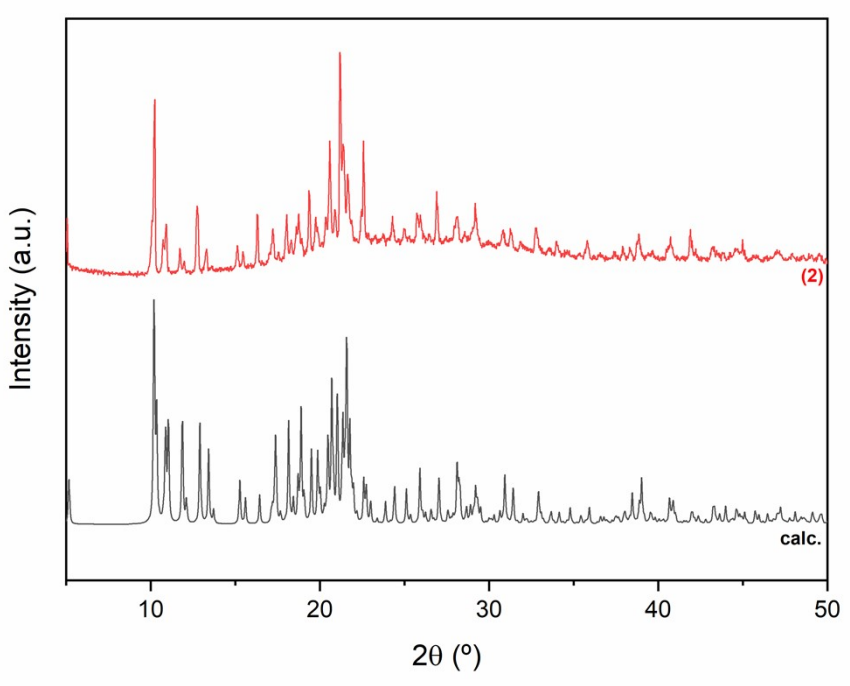

Figure S4. Experimental (red) and calculated (black) PXRD patterns for **2**.

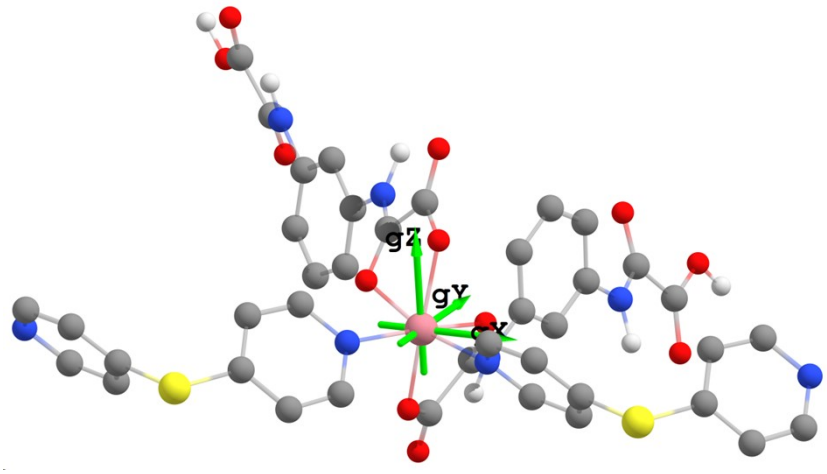

Figure S5. Calculated structure of the Co(II) in **(1)** showing the orientation of the principal axes of the g-tensor (g_x, g_y, g_z) for the ground S = 3/2 multiplet. Color code: Co, pink; C, grey; N, blue; O, red; S, yellow; H, white.

(a)

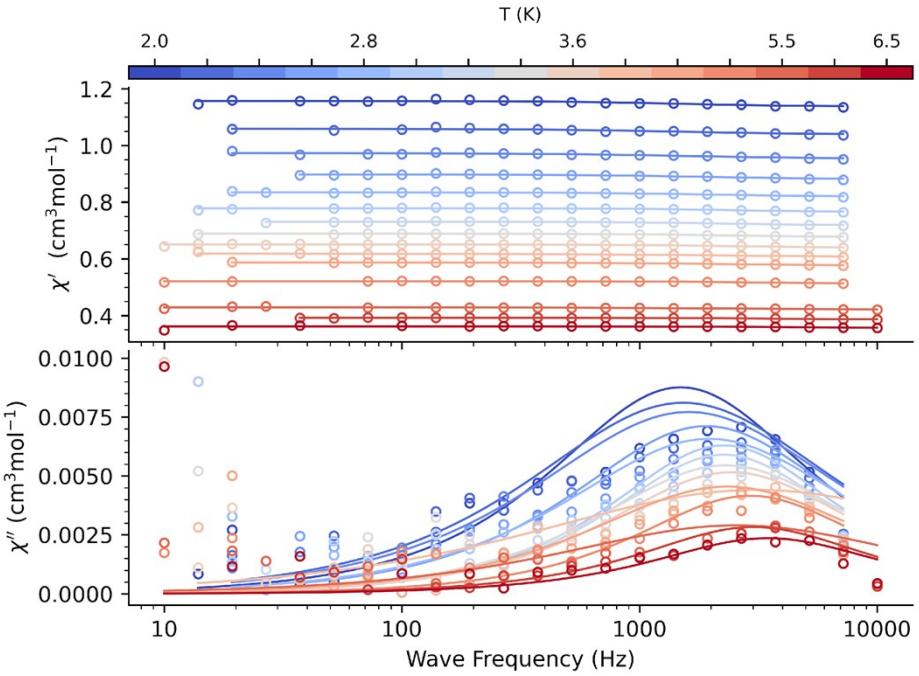
T (K)
2.0
2.8
3.6
5.5
6.5
1.2
1.0
0.8
0.6
0.4
χ′ (cm³mol⁻¹)
0.0100
0.0075
0.0050
0.0025
0.0000
χ″ (cm³mol⁻¹)
10
100
1000
10000
Wave Frequency (Hz)

(b)

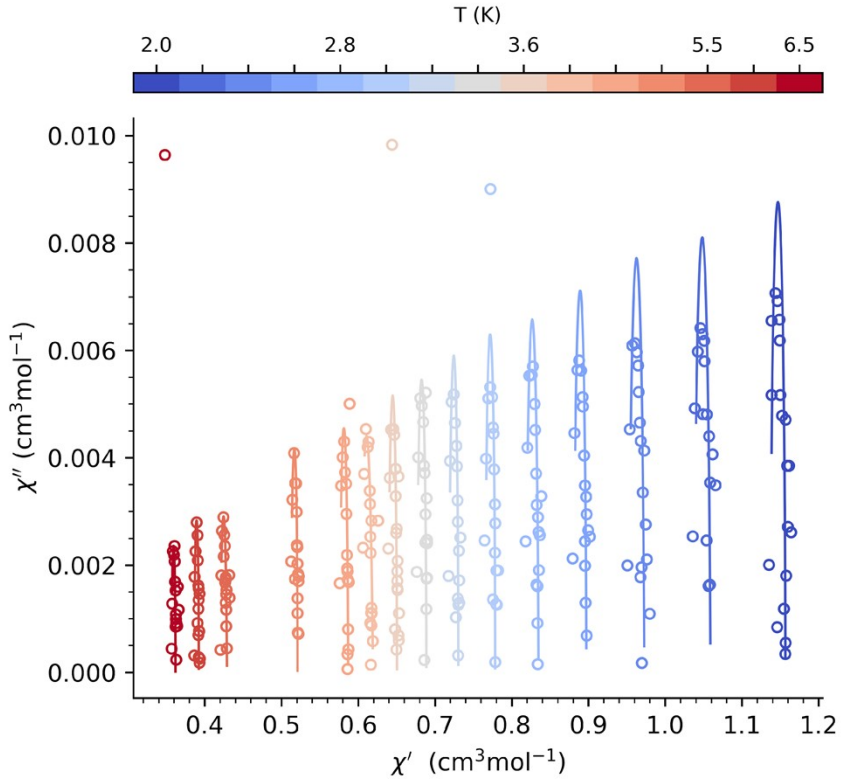
T (K)
2.0
2.8
3.6
5.5
6.5
0.010
0.008
0.006
0.004
0.002
0.000
χ″ (cm³mol⁻¹)
0.4
0.5
0.6
0.7
0.8
0.9
1.0
1.1
1.2
χ′ (cm³mol⁻¹)

Figure S6. (a) Frequency dependence of the ac susceptibility for **1**, measured in the absence of a magnetic field. (b) Cole-Cole plot obtained from the frequency-dependence of the ac susceptibility for **1** measured in the absence of a magnetic field. Lines represent the best-fit curves obtained using a generalized Debye model with one relaxation process according to the description in the text.

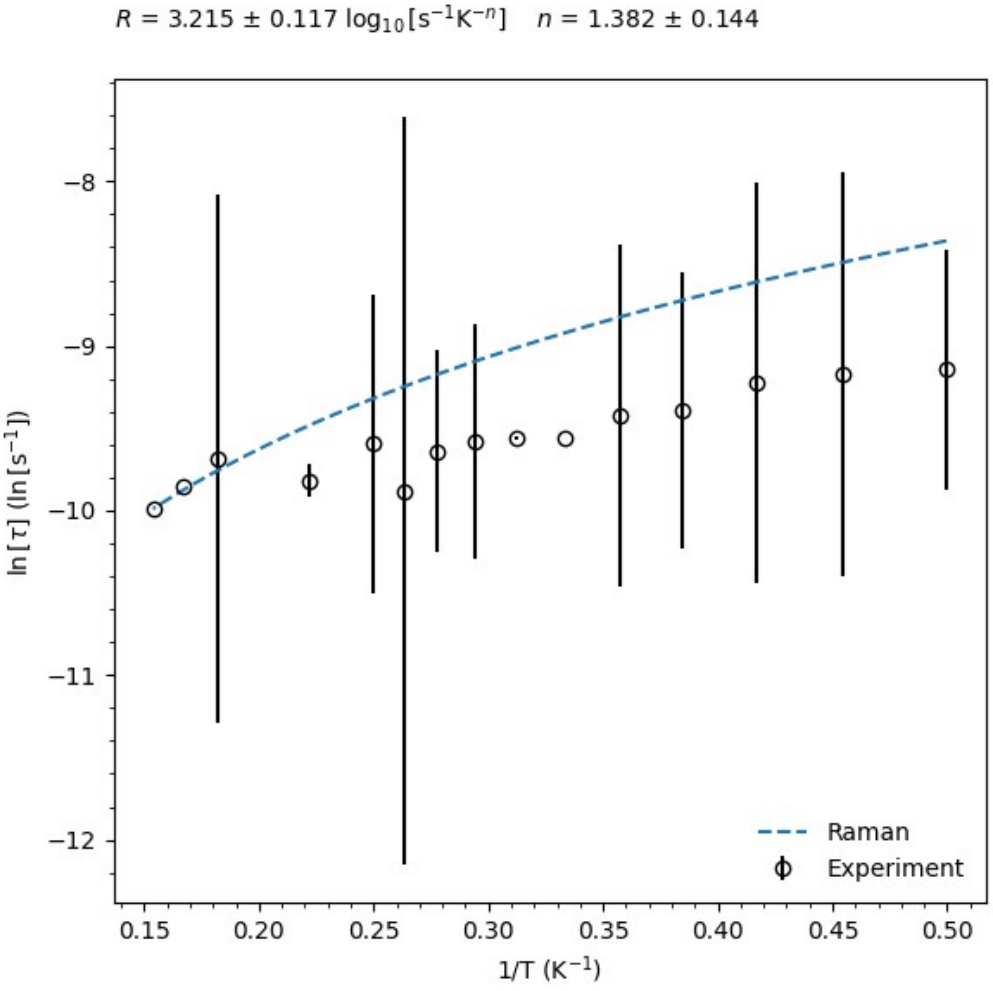

Figure S7. Arrhenius-like plot lnτ vs. $T^{-1.}$ Temperature dependence of the relaxation time for the compound **1**. (– fitted by model Raman, black). (measured in the absence of a magnetic field).

REFERENCES

1. Y.Z. Zheng, M. Speldrich, H. Schilder, X.M. Chen, P. Kögerler, A tetranuclear cobalt(II) chain with slow magnetization relaxation, *Dalton Transactions*, **2010**, 39(45), 10827–10829.
2. W. Huang, T. Liu, D. Wu, J. Cheng, Z.W. Ouyang, C. Duan, Field-induced slow relaxation of magnetization in a tetrahedral Co(II) complex with easy plane anisotropy, *Dalton Transactions*, **2013**, 42(43), 15326–15331.
3. L. Smolko, J. Černák, M. Dušek, J. Miklovič, J. Titiš, R. Boča, Three tetracoordinate Co(II) complexes $[Co(biq)X_2]$ (X = Cl, Br, I) with easy-plane magnetic anisotropy as field-induced single-molecule magnets, *Dalton Transactions*, **2015**, 44(40), 17565–17571.
4. D. Tu, D. Shao, H. Yan, C. Lu, A carborane-incorporated mononuclear Co(II) complex showing zero-field slow magnetic relaxation, *Chemical Communications*, **2016**, 52(99), 14326–14329.
5. S. Roy, I. Oyarzabal, J. Vallejo, J. Cano, E. Colacio, A. Bauza, A. Frontera, A.M. Kirillov, M.G.B. Drew, S. Das, Two Polymorphic Forms of a Six-Coordinate Mononuclear Cobalt(II) Complex with Easy-Plane Anisotropy: Structural Features, Theoretical Calculations, and Field-Induced Slow Relaxation of the Magnetization, *Inorganic Chemistry*, **2016**, 55(17), 8502–8513.
6. L. Smolko, J. Černák, J. Kuchár, C. Rajnák, J. Titiš, R. Boča, Field-Induced Slow Magnetic Relaxation in Mononuclear Tetracoordinate Cobalt(II) Complexes Containing a Neocuproine Ligand, *European Journal of Inorganic Chemistry*, **2017**, 2017(24), 3080–3086.
7. F. Shao, B. Cahier, E. Rivière, R. Guillot, N. Guihéry, V.E. Campbell, T. Mallah, Structural Dependence of the Ising-type Magnetic Anisotropy and of the

Relaxation Time in Mononuclear Trigonal Bipyramidal Co(II) Single Molecule Magnets, *Inorganic Chemistry*, **2017**, 56(3), 1104–1111.

8. F. El-Khatib, B. Cahier, F. Shao, M. López-Jordà, R. Guillot, E. Rivière, H. Hafez, Z. Saad, J.J. Girerd, N. Guihéry, T. Mallah, Design and Magnetic Properties of a Mononuclear Co(II) Single Molecule Magnet and Its Antiferromagnetically Coupled Binuclear Derivative, *Inorganic Chemistry*, **2017**, 56(8), 4601–4608.
9. X.F. Ma, Z. Wang, X.L. Chen, M. Kurmoo, M.H. Zeng, Ligand Effect on the Single-Molecule Magnetism of Tetranuclear Co(II) Cubane, *Inorganic Chemistry*, **2017**, 56(24), 15178–15186.
10. R. Mitsuhashi, K.S. Pedersen, T. Ueda, T. Suzuki, J. Bendix, M. Mikuriya, Field-induced single-molecule magnet behavior in ideal trigonal antiprismatic cobalt(II) complexes: precise geometrical control by a hydrogen-bonded rigid metalloligand, *Chemical Communications*, **2018**, 54(64), 8869–8872.
11. D. Shao, L. Shi, L. Yin, B.L. Wang, Z.X. Wang, Y.Q. Zhang, X.Y. Wang, Reversible on-off switching of both spin crossover and single-molecule magnet behaviours: Via a crystal-to-crystal transformation, *Chemical Science*, **2018**, 9(41), 7986–7991.
12. V. García-López, F.J. Orts-Mula, M. Palacios-Corella, J.M. Clemente-Juan, M. Clemente-León, E. Coronado, Field-induced slow relaxation of magnetization in a mononuclear Co(II) complex of 2,6-bis(pyrazol-1-yl)pyridine functionalized with a carboxylic acid, *Polyhedron*, **2018**, 150, 54–60.
13. A.K. Mondal, A. Mondal, B. Dey, S. Konar, Influence of the Coordination Environment on Easy-Plane Magnetic Anisotropy of Pentagonal Bipyramidal Cobalt(II) Complexes, *Inorganic Chemistry*, **2018**, 57(16), 9999–10008.

14. L. Váhovská, O. Bukrynov, I. Potočňák, E. Čižmár, A. Kliuikov, S. Vitushkina, M. Dušek, R. Herchel, New Cobalt(II) Field-Induced Single-Molecule Magnet and the First Example of a Cobalt(III) Complex with Tridentate Binding of a Deprotonated 4-Amino-3,5-bis(pyridin-2-yl)-1,2,4-Triazole Ligand, *European Journal of Inorganic Chemistry*, **2019**, 2019(2), 250–261.
15. D. Valigura, C. Rajnák, J. Moncol, J. Titiš, R. Boča, A mononuclear Co(II) complex formed from pyridinedimethanol with manifold slow relaxation channels, *Dalton Transactions*, **2017**, 46(33), 10950–10956.
16. T. Ishizaki, T. Fukuda, M. Akaki, A. Fuyuhiro, M. Hagiwara, N. Ishikawa, Synthesis of a Neutral Mononuclear Four-Coordinate Co(II) Complex Having Two Halved Phthalocyanine Ligands That Shows Slow Magnetic Relaxations under Zero Static Magnetic Field, *Inorganic Chemistry*, **2019**, 58(8), 5211–5220.
17. H. Zenno, R. Akiyoshi, M. Nakamura, G.G. Morgan, S. Hayami, Orbital angular momentum crossover in 1-D High Spin Cobalt(II) complex, *Chemistry Letters*, **2020**, 49(9), 1099–1102.
18. E. Zahradníková, R. Herchel, I. Šalitroš, I. Císařová, B. Drahoš, Late first-row transition metal complexes of a 17-membered piperazine-based macrocyclic ligand: Structures and magnetism, *Dalton Transactions*, **2020**, 49(26), 9057–9069.
19. L.D.S. Mariano, I.M.L. Rosa, N.R. de Campos, A.C. Doriguetto, D.F. Dias, W.D. do Pim, A.K.S.M. Valdo, F.T. Martins, M.A. Ribeiro, E.E.B. de Paula, E.F. Pedroso, H.O. Stumpf, J. Cano, F. Lloret, M. Julve, M.V. Marinho, Polymorphic Derivatives of Ni^{II} and Co^{II} Mesocates with 3D Networks and “brick and mortar” Structures: Preparation, Structural Characterization, and Cryomagnetic

Investigation of New Single-Molecule Magnets, *Crystal Growth and Design*, **2020**, 20(4), 2462–2476.

20. A. Landart-Gereka, M.M. Quesada-Moreno, I.F. Díaz-Ortega, H. Nojiri, M. Ozerov, J. Krzystek, M.A. Palacios, E. Colacio, Large easy-axis magnetic anisotropy in a series of trigonal prismatic mononuclear cobalt(II) complexes with zero-field hidden single-molecule magnet behaviour: the important role of the distortion of the coordination sphere and intermolecular interactions in the slow relaxation, *Inorganic Chemistry Frontiers*, **2022**, 9(12), 2810–2831.
21. R. Akiyoshi, H. Zenno, Y. Sekine, M. Nakaya, M. Akita, D. Kosumi, L.F. Lindoy, S. Hayami, A Ferroelectric Metallomesogen Exhibiting Field-Induced Slow Magnetic Relaxation, *Chemistry - A European Journal*, **2022**, 28(5).
22. B. Yao, Y.Q. Zhang, Y.F. Deng, T. Li, Y.Z. Zhang, Series of Benzoquinone-Bridged Dicobalt(II) Single-Molecule Magnets, *Inorganic Chemistry*, **2022**, 61(39), 15392–15397.
23. Y.L. Wang, L. Chen, C.M. Liu, Y.Q. Zhang, S.G. Yin, Q.Y. Liu, Field-Induced Slow Magnetic Relaxation and Gas Adsorption Properties of a Bifunctional Cobalt(II) Compound, *Inorganic Chemistry*, **2015**, 54(23), 11362–11368.
24. J. Vallejo, F.R. Fortea-Pérez, E. Pardo, S. Benmansour, I. Castro, J. Krzystek, D. Armentano, J. Cano, Guest-dependent single-ion magnet behaviour in a cobalt(II) metal-organic framework, *Chemical Science*, **2016**, 7(3), 2286–2293.
25. D. Shao, L. Shi, S.L. Zhang, X.H. Zhao, D.Q. Wu, X.Q. Wei, X.Y. Wang, Syntheses, structures, and magnetic properties of three new chain compounds based on a pentagonal bipyramidal Co(II) building block, *CrystEngComm*, **2016**, 18(22), 4150–4157.

26. A.V. Palii, D.V. Korchagin, E.A. Yureva, A.V. Akimov, E.Y. Misochko, G.V. Shilov, A.D. Talantsev, R.B. Morgunov, S.M. Aldoshin, B.S. Tsukerblat, Single-Ion Magnet $Et_4N[Co^{II}(hfac)_3]$ with Nonuniaxial Anisotropy: Synthesis, Experimental Characterization, and Theoretical Modeling, *Inorganic Chemistry*, **2016**, 55(19), 9696–9706.
27. A. Świtlicka, B. Machura, R. Kruszynski, J. Cano, L.M. Toma, F. Lloret, M. Julve, The influence of pseudohalide ligands on the SIM behaviour of four-coordinate benzylimidazole-containing cobalt(II) complexes, *Dalton Transactions*, **2018**, 47(16), 5831–5842.
28. S. Vaidya, P. Shukla, S. Tripathi, E. Rivière, T. Mallah, G. Rajaraman, M. Shanmugam, Substituted versus Naked Thiourea Ligand Containing Pseudotetrahedral Cobalt(II) Complexes: A Comparative Study on Its Magnetization Relaxation Dynamics Phenomenon, *Inorganic Chemistry*, **2018**, 57(6), 3371–3386.
29. X.X. Jin, X.X. Chen, J. Xiang, Y.Z. Chen, L.H. Jia, B.W. Wang, S.C. Cheng, X. Zhou, C.F. Leung, S. Gao, Slow magnetic relaxation in a series of mononuclear 8-coordinate Fe(II) and Co(II) complexes, *Inorganic Chemistry*, **2018**, 57(7), 3761–3774.
30. M. Roy, A. Adhikary, A.K. Mondal, R. Mondal, Multifunctional Properties of a 1D Helical Co(II) Coordination Polymer: Toward Single-Ion Magnetic Behavior and Efficient Dye Degradation, *ACS Omega*, **2018**, 3(11), 15315–15324.
31. F. Kobayashi, R. Ohtani, M. Nakamura, L.F. Lindoy, S. Hayami, Slow Magnetic Relaxation Triggered by a Structural Phase Transition in Long-Chain-Alkylated Cobalt(II) Single-Ion Magnets, *Inorganic Chemistry*, **2019**, 58(11), 7409–7415.

32. J. Vallejo, M. Viciano-Chumillas, F. Lloret, M. Julve, I. Castro, J. Krzystek, M. Ozerov, D. Armentano, G. de Munno, J. Cano, Coligand Effects on the Field-Induced Double Slow Magnetic Relaxation in Six-Coordinate Cobalt(II) Single-Ion Magnets (SIMs) with Positive Magnetic Anisotropy, *Inorganic Chemistry*, **2019**, 58(23), 15726–15740.
33. G. Yi, H. Cui, C. Zhang, W. Zhao, L. Chen, Y.Q. Zhang, X.T. Chen, Y. Song, A. Yuan, A capped trigonal prismatic cobalt(II) complex as a structural archetype for single-ion magnets, *Dalton Transactions*, **2020**, 49(7), 2063–2067.
34. Y.P. Tupolova, I.N. Shcherbakov, D.V. Korchagin, V.V. Tkachev, V.E. Lebedev, L.D. Popov, K.V. Zakharov, A.N. Vasiliev, A.V. Palii, S.M. Aldoshin, Fine-Tuning of Uniaxial Anisotropy and Slow Relaxation of Magnetization in the Hexacoordinate Co(II) Complexes with Acidoligands, *Journal of Physical Chemistry C*, **2020**, 124(47), 25957–25966.
35. P.S. Ferreira, J.F. Malta, N.A.G. Bandeira, A. Allgaier, J. van Slageren, J.A. Paixão, M. Almeida, L.C.J. Pereira, P.T. Gomes, Enhancing SIM behaviour in a mononuclear tetrahedral [Co(N,N′-2-iminopyrrolyl)$_2$] complex, *Chemical Communications*, **2022**, 58(69), 9682–9685.
36. Z. Xia, Y. Li, C. Ji, Y. Jiang, C. Ma, J. Gao, J. Zhang, Slow-Relaxation Behavior of a Mononuclear Co(II) Complex Featuring Long Axial Co-O Bond, *Nanomaterials*, **2022**, 12(4).
37. D. Shao, S. Moorthy, P. Peng, W.J. Tang, L. Shi, Z.J. Wang, X.Q. Wei, S. Kumar Singh, A Single-Ion Magnet Tape with Five-Coordinate Cobalt(II) Centers, *European Journal of Inorganic Chemistry*, **2022**, 2022(27).

38. W.J. Tang, S.T. Wu, X.M. Bu, H.Y. Zhang, X.Q. Wei, D. Shao, Field-induced single-ion magnet behavior in a cobalt(II) coordination polymer constructed by a mixed bipyridyl-tetracarboxylate strategy, *Polyhedron*, **2023**, 229, 116175.
39. S.K. Gupta, H.H. Nielsen, A.M. Thiel, E.A. Klahn, E. Feng, H.B. Cao, T.C. Hansen, E. Lelièvre-Berna, A. Gukasov, I. Kibalin, S. Dechert, S. Demeshko, J. Overgaard, F. Meyer, Multi-Technique Experimental Benchmarking of the Local Magnetic Anisotropy of a Cobalt(II) Single-Ion Magnet, *JACS Au*, **2023**, 3(2), 429–440.
40. G. Bhatt, T. Sharma, S.K. Gupta, F. Meyer, G. Rajaraman, R. Murugavel, Tuning Magnetic Anisotropy in Co(II) Tetrahedral Carbazole-Modified Phosphine Oxide Single-Ion Magnets: Importance of Structural Distortion versus Heavy-Ion Effect, *Inorganic Chemistry*, **2023**, 62(46), 18915–18925.
41. Y. Cui, Y. Xu, X. Liu, Y. Li, B.L. Wang, Y. Dong, W. Li, S. Lei, Field-Induced Single-Ion Magnetic Behavior in Two Mononuclear Cobalt(II) Complexes, *Chemistry - An Asian Journal*, **2019**, 14(15), 2620–2628.
42. H.H. Cui, Y.Q. Zhang, X.T. Chen, Z. Wang, Z.L. Xue, Magnetic anisotropy and slow magnetic relaxation processes of cobalt(II)-pseudohalide complexes, *Dalton Transactions*, **2019**, 48(28), 10743–10752.
43. J. Palion-Gazda, T. Klemens, B. Machura, J. Vallejo, F. Lloret, M. Julve, Single ion magnet behaviour in a two-dimensional network of dicyanamide-bridged cobalt(II) ions, *Dalton Transactions*, **2015**, 44(7), 2989–2992.
44. A.K. Mondal, S. Khatua, K. Tomar, S. Konar, Field-Induced Single-Ion-Magnetic Behavior of Octahedral CoIIin a Two-Dimensional Coordination Polymer, *European Journal of Inorganic Chemistry*, **2016**, 2016(22), 3545–3552.

45. X. Liu, L. Sun, H. Zhou, P. Cen, X. Jin, G. Xie, S. Chen, Q. Hu, Single-Ion-Magnet Behavior in a Two-Dimensional Coordination Polymer Constructed from Co^{II} Nodes and a Pyridylhydrazone Derivative, *Inorganic Chemistry*, **2015**, 54(18), 8884–8886.
46. J. Vallejo, I. Castro, R. Ruiz-García, J. Cano, M. Julve, F. Lloret, G. de Munno, W. Wernsdorfer, E. Pardo, Field-induced slow magnetic relaxation in a six-coordinate mononuclear cobalt(II) complex with a positive anisotropy, *Journal of the American Chemical Society*, **2012**, 134(38), 15704–15707.
47. L. Shi, F.X. Shen, D. Shao, Y.Q. Zhang, X.Y. Wang, Syntheses, structures, and magnetic properties of three two-dimensional cobalt(II) single-ion magnets with a $Co^{II}N_4X_2$ octahedral geometry, *CrystEngComm*, **2019**, 21(20), 3176–3185.
48. H.V.P. Hollauer, G.S. de Araújo, G.P. Guedes, H.C.S. Junior, S. Letichevsky, L. Ghivelder, S. Soriano, O. Cambraia, L.B.L. Escobar, Synthesis, crystal structure and magnetic properties of two 1D coordination polymers containing Co^{2+} and Cu^{2+} ions and 1,3,5-tris(4-carboxylphenyl)benzene, *Journal of Molecular Structure*, **2024**, 1306, 137811.
49. N.R. de Campos, C.A. Simosono, I.M. Landre Rosa, R.M.R. da Silva, A.C. Doriguetto, W.D. do Pim, T.R. Gomes Simões, A.K.S.M. Valdo, F.T. Martins, C.V. Sarmiento, W.C. Nunes, G.P. Guedes, E.F. Pedroso, C.L.M. Pereira, H.O. Stumpf, F. Lloret, M. Julve, M.V. Marinho, Building-up host-guest helicate motifs and chains: a magneto-structural study of new field-induced cobalt-based single-ion magnets, *Dalton Transactions*, **2021**, 50(31), 10707–10728.
50. A. Świtlicka-Olszewska, J. Palion-Gazda, T. Klemens, B. Machura, J. Vallejo, J. Cano, F. Lloret, M. Julve, Single-ion magnet behaviour in mononuclear and two-

dimensional dicyanamide-containing cobalt(II) complexes, *Dalton Transactions*, **2016**, 45(25), 10181–10193.

51. J.P.S. Walsh, G. Bowling, A.M. Ariciu, N.F.M. Jailani, N.F. Chilton, P.G. Waddell, D. Collison, F. Tuna, L.J. Higham, Evidence of slow magnetic relaxation in $Co(AcO)_2(py)_2(H_2O)_2$, *Magnetochemistry*, **2016**, 2(2).
52. C. Rajnák, J. Titiš, J. Moncoľ, F. Renz, R. Boča, Field-Supported Slow Magnetic Relaxation in Hexacoordinate Co^{II} Complexes with Easy Plane Anisotropy, *European Journal of Inorganic Chemistry*, **2017**, 2017(11), 1520–1525.
53. T.T. da Cunha, V.M.M. Barbosa, W.X.C. Oliveira, E.F. Pedroso, D.M.A. Garciá, W.C. Nunes, C.L.M. Pereira, Field-Induced Slow Magnetic Relaxation of a Six-Coordinate Mononuclear Manganese(II) and Cobalt(II) Oxamate Complexes, *Inorganic Chemistry*, **2020**, 59(18), 12983–12987.
54. L. Croitor, E.B. Coropceanu, A. V. Siminel, O. Kulikova, V.I. Zelentsov, T. Datsko, M.S. Fonari, 1,2-Cyclohexanedionedioxime as a useful co-ligand for fabrication of one-dimensional Zn(II) and Cd(II) coordination polymers with wheel-and-axle topology and luminescent properties, *CrystEngComm*, **2012**, 14, 3750-3758.
55. M.V. Marinho, L.F. Marques, R. Diniz, H.O. Stumpf, L. do Canto Visentin, M.I. Yoshida, F.C. Machado, F. Lloret, M. Julve, Solvothermal synthesis, crystal structure and magnetic properties of homometallic Co(II) and Cu(II) chains with double di(4-pyridyl)sulfide as bridges, *Polyhedron*, **2012**, 45, 1–8.
56. C.R. Maldonado, M. Quirós, J.M. Salas, H-bonds superstructures built by aquacomplexes and an azapurine derivative: a case of molecular recognition, *Dalton Transactions*, **2012**, 41, 10390-10395.

57. Y.-M. Yang, X.-X. Cao, T.-T. Lv, Y. Song, Crystal structure of diaquabis[μ-3-(4-carboxylatophenyl) propionato]bis(μ-4,4'-thiodipyridine)dinickel(II), $Ni_2(H_2O)_2(C_{10}H_8O_4)_2(C_{10}H_8N_2S)_2$, *Zeitschrift Für Kristallographie - New Crystal Structures*, **2012**, 227, 129-130.

58. J.-X. Li, Z.-X. Du, Syntheses, Structures and fluorescent properties of copper(II) and manganese(II) helical complexes bridged by 4,4′-Dipyridylsulfide, *Chinese J. Struct. Chem.*, **2012**, 31, 877–883.

59. J.-H. Qin, J.-G. Wang, Y. Hu, L.-F. Ma, Synthesis and crystal structure of a new cobalt complex based on 5-bromoisophthalate and 4,4'-dipyridyldisulfide ligands, *Synthesis and Reactivity in Inorganic, Metal-Organic, and Nano-Metal Chemistry*, **2013**, 43, 552–555.

60. M.-L. Han, X.-H. Chang, X.-J. Wu, A new zinc(II) coordination polymer based on 5-methylisophthalic acid and 4,4′-dipyridylsulfide: synthesis, structure, and photoluminescent properties, *Synthesis and Reactivity in Inorganic, Metal-Organic, and Nano-Metal Chemistry*, **2013**, 43, 479–482.

61. M.-L. Han, Z.-Z. Shi, F.-F. Li, Two new Co(II) complexes based on dicarboxylate linker and N-donors ligands: syntheses and crystal structures, *Synthesis and Reactivity in Inorganic, Metal-Organic, and Nano-Metal Chemistry*, **2013**, 43, 892–896.

62. Y. Zhao, J.-H. Qin, L.-F. Ma, L.-Y. Wang, Synthesis and crystal structure of a porous framework obtained by *in situ* ligand formation from 4,4′-dipyridyldisulfide, *Synthesis and Reactivity in Inorganic, Metal-Organic, and Nano-Metal Chemistry*, **2013**, 43, 864–868.

63. J. Zhao, D.-S. Li, Y.-P. Wu, J.-J. Yang, W.-W. Dong, K. Zou, A rare pentanuclear CuII-based coordination framework exhibiting coexistence of

antiferromagnetic and ferromagnetic couplings, *Inorg Chem Commun*, **2013**, 35, 61–64.

64. H.-L. Jia, M.-J. Jia, G.-H. Li, Y.-N. Wang, J.-H. Yu, J.-Q. Xu, New thiocyanatocadmates templated by multi-dentate N-heterocyclic/diamine molecules, *Dalton Transactions*, **2013**, 42, 6429-6439.
65. L.Y. Xin, G.Z. Liu, X.L. Li, H. Guo, Dipyridyl-type ligand-directed assembly of three cobalt(II) coordinated polymers based on carboxyphenylpropionate, *Russian Journal of Coordination Chemistry*, **2013**, 39, 571–578.
66. L. Croitor, E.B. Coropceanu, D. Chisca, S.G. Baca, J. van Leusen, P. Kögerler, P. Bourosh, V.Ch. Kravtsov, D. Grabco, C. Pyrtsac, M.S. Fonari, Effects of anion and bipyridyl bridging ligand identity on the Co(II) coordination networks, *Cryst Growth Des*, **2014**, 14, 3015–3025.
67. S.C. Manna, S. Mistri, E. Zangrando, Synthesis, crystal structure, solid state electronic spectra and thermal study of three cobalt(II)–selenocyanate complexes: *In situ* room temperature transformation of 4,4′-dipyridyldisulfide to 4,4′-dipyridylsulfide, *Inorganica Chim Acta*, **2014**, 413, 166–173.
68. J.-G. Wang, J.-H. Qin, L. Li, L.-F. Ma, Two Mn(II)/Co(II) coordination polymers involving 4,4′-dipyridyltrisulfide/4,4′-dipyridylsulfide obtained by *in situ* ligand formation from 4,4′-dipyridyldisulfide, *Synthesis and Reactivity in Inorganic, Metal-Organic, and Nano-Metal Chemistry*, **2014**, 44, 112–117.
69. D. Yang, H. Zhou, A.-H. Yuan, Y.-Z. Li, Sandwich-like octacyanometalate-based cadmium assemblies with the 4,4′-dipyridyl sulfide ligand, *CrystEngComm*, **2014**, 16, 8344–8347.

70. L. Tang, L. Gao, F. Fu, J. Cao, D. Chao, Two 1D coordination polymers constructed from copper(II) carboxylates and 4,4′-dipyridyl sulfide/4,4′-dipyridyl disulfide, *Z Anorg Allg Chem*, **2014**, 640, 1368–1373.
71. N. de la Pinta, A.B. Caballero, G. Madariaga, J.M. Ezpeleta, A. Rodriguez-Dieguez, J.M. Salas, R. Cortés, DPDS–DPS *in situ* transformation at room temperature via a 1,2-nucleophilic addition mechanism, *CrystEngComm*, **2014**, 16, 8322–8326.
72. L. Zhu, Y.-S. Hu, L.-H. Zhu, Z. An, Solvothermal *in situ* ligand synthesis to fabricate a new luminescent Cu(I) coordination polymer, *Synthesis and Reactivity in Inorganic, Metal-Organic, and Nano-Metal Chemistry*, **2014**, 44, 1469–1472.
73. W. Liu, Y. Fang, G.Z. Wei, S.J. Teat, K. Xiong, Z. Hu, W.P. Lustig, J. Li, A family of highly efficient CuI-based lighting phosphors prepared by a systematic, bottom-up synthetic approach, *J Am Chem Soc*, **2015**, 137, 9400–9408.
74. B. Ugale, D. Singh, C.M. Nagaraja, Temperature dependent structural variation from 2D supramolecular network to 3D interpenetrated metal–organic framework: In situ cleavage of S–S and C–S bonds, *J Solid State Chem*, **2015**, 226, 273–278.
75. J.-H. Qin, S.-J. Liu, H.-R. Wang, A coordination polymer involving two different binuclear Co(II) clusters obtained by *in situ* ligand formation from 4,4′-dipyridyldisulfide, *Synthesis and Reactivity in Inorganic, Metal-Organic, and Nano-Metal Chemistry*, **2015**, 45, 68–73.
76. H.B. Wang, Y.P. Wu, G.W. Xu, J.F. Wang, S.S. Guo, Three new Co(II)/Ni(II) coordination polymers based on 3,3-biphenyl dicarboxylic acid and N-donor Co-ligands: Synthesis, crystal structures and magnetic properties, *Russian Journal of Coordination Chemistry*, **2015**, 41, 664–672.

77. M.-L. Han, L. Bai, P. Tang, X.-Q. Wu, Y.-P. Wu, J. Zhao, D.-S. Li, Y.-Y. Wang, Biphenyl-2,4,6,3′,5′-pentacarboxylic acid as a tecton for six new Co(II) coordination polymers: pH and N-donor ligand-dependent assemblies, structure diversities and magnetic properties, *Dalton Transactions*, **2015**, 44, 14673–14685.

78. N.R. de Campos, M.A. Ribeiro, W.X.C. Oliveira, D.O. Reis, H.O. Stumpf, A.C. Doriguetto, F.C. Machado, C.B. Pinheiro, F. Lloret, M. Julve, J. Cano, M. V. Marinho, Magneto-structural versatility of copper(II)-3-phenylpropionate coordination polymers with N-donor coligands, *Dalton Transactions*, **2016**, 45, 172–189.

79. R.-B. Lin, L. Li, H. Wu, H. Arman, B. Li, R.-G. Lin, W. Zhou, B. Chen, Optimized separation of acetylene from carbon dioxide and ethylene in a microporous material, *J Am Chem Soc*, **2017**, 139, 8022–8028.

80. S. Sanram, J. Boonmak, S. Youngme, Structural diversity, single-crystal to single-crystal transformation and photocatalytic properties of Cu(II)-metal-organic frameworks based on 1,4-phenylenedipropionic acid, *Inorganica Chim Acta*, **2018**, 469, 11–19.

81. M.-Y. Chao, J. Chen, D.J. Young, W.-H. Zhang, J.-P. Lang, Smoothing the single-crystal to single-crystal conversions of a two-dimensional metal–organic framework *via* the hetero-metal doping of the linear trimetallic secondary building unit, *Dalton Transactions*, **2018**, 47, 13722–13729.

82. N.V. Reis, M.V. Marinho, T.R.G. Simões, K.C. Metz, R.C.A. Vaz, W.X.C. Oliveira, C.L.M. Pereira, W.P. Barros, C.B. Pinheiro, S.O.K. Giese, D.L. Hughes, K.R. Pirota, W.C. Nunes, H.O. Stumpf, Structural versatility driven by the flexible

di(4-pyridyl) sulfide ligand: From cobalt(II) single-ion magnets to sheet-like copper(II) weak antiferromagnets, *Polyhedron*, **2019**, 171, 203–211.

83. A.N. Morozov, L.D. Popov, V. V. Tkachev, E.A. Raspopova, V.A. Chetverikova, S.N. Lyubchenko, G. V. Shilov, Synthesis and crystal structure of 2D coordination polymer $\{[Cu(dps)_2(DMSO)_2](ClO_4)_2\}_n$ based on 4,4′-dipyridyl sulfide, *Russ J Gen Chem*, **2019**, 89, 82–86.
84. M.-Y. Chao, J. Chen, Z.-M. Hao, X.-Y. Tang, L. Ding, W.-H. Zhang, D.J. Young, J.-P. Lang, A single-crystal to single-crystal conversion scheme for a two-dimensional metal–organic framework bearing linear Cd_3 secondary building units, *Cryst Growth Des*, **2019**, 19, 724–729.
85. Y. Wang, X. Jia, H. Yang, Y. Wang, X. Chen, A.N. Hong, J. Li, X. Bu, P. Feng, A strategy for constructing pore-space-partitioned MOFs with high uptake capacity for C_2 hydrocarbons and CO_2, *Angewandte Chemie International Edition*, **2020**, 59, 19027–19030.
86. J. Wang, Y. Zhang, P. Zhang, J. Hu, R.-B. Lin, Q. Deng, Z. Zeng, H. Xing, S. Deng, B. Chen, Optimizing pore space for flexible-robust metal–organic framework to boost trace acetylene removal, *J Am Chem Soc*, **2020**, 142, 9744–9751.
87. X.-G. Yang, Z.-M. Zhai, X.-Y. Liu, J.-Y. Li, F.-F. Li, L.-F. Ma, Sulfur heteroatom-based MOFs with long-lasting room-temperature phosphorescence and high photoelectric response, *Dalton Transactions*, **2020**, 49, 598–602.
88. X.-H. Chang, Z.-M. Zhai, X.-M. Lu, Crystal structure of tetraaqua-bis(μ_2-5-aminoisophthalato-κ^3N:*O*,*O*′)-bis(4,4′-dipyridylsulfide-κ^1N)dizinc(II), $C_{36}H_{34}N_6O_{12}S_2Ni_2$, *Zeitschrift Für Kristallographie - New Crystal Structures*, **2020**, 235, 73–75.

89. J. Shen, X. He, T. Ke, R. Krishna, J.M. van Baten, R. Chen, Z. Bao, H. Xing, M. Dincă, Z. Zhang, Q. Yang, Q. Ren, Simultaneous interlayer and intralayer space control in two-dimensional metal−organic frameworks for acetylene/ethylene separation, *Nat Commun*, **2020**, 11, 6259.
90. Y. Zhao, L.-L. Dang, Z.-M. Zhai, L.-F. Ma, L.-Y. Wang, Crystal structures and magnetic properties of two Co(II) coordination polymers created via in situ ligand synthesis, *J Solid State Chem*, **2020**, 290, 121573.
91. T. Ke, Q. Wang, J. Shen, J. Zhou, Z. Bao, Q. Yang, Q. Ren, molecular sieving of C_2-C_3 alkene from alkyne with tuned threshold pressure in robust layered metal–organic frameworks, *Angewandte Chemie International Edition*, **2020**, 59, 12725–12730.
92. N.-H. Huang, Y. Liu, R.-T. Li, J. Chen, P.-P. Hu, D.J. Young, J.-X. Chen, W.-H. Zhang, Sequential Ag^+/biothiol and synchronous Ag^+/Hg^{2+} biosensing with zwitterionic Cu^{2+}-based metal–organic frameworks, *Analyst*, **2020**, 145, 2779–2788.
93. J. Wang, Y. Zhang, Y. Su, X. Liu, P. Zhang, R.-B. Lin, S. Chen, Q. Deng, Z. Zeng, S. Deng, B. Chen, Fine pore engineering in a series of isoreticular metal-organic frameworks for efficient C_2H_2/CO_2 separation, *Nat Commun*, **2022**, 13, 200.
94. L.-H. Li, Y. Peng, S. Zhang, T. Xiao, Y. Song, H.-Y. Ye, J. Zhang, Y.-Q. Zhang, Z. Wang, Z.-B. Hu, Effect of subtle changes on the slow relaxation behavior of Co(II) ions based metal-organic frameworks, *Cryst Growth Des*, **2023**, 23, 2099–2105.

95. B. Tan, Z.-F. Wu, M.-Z. Jia, J. Zhang, G.-Y. Yang, Confinement of pyridine derivatives into a metal–organic framework host as electron acceptors to achieve photoinduced electron-transfer, *Inorg Chem*, **2023**, 62, 6688–6695.

96. R. Carballo, N. Fernández-Hermida, A.B. Lago, S. Rodríguez-Hermida, E.M. Vázquez-López, Supramolecular networks through second-sphere coordination based on 1D metal-4,4′-dipyridyldisulfide coordination polymers and hydrogenfumarate or sulfonate anions, *Polyhedron*, **2012**, 31, 118–127.

97. I.H. Hwang, Y.D. Jo, H.-Y. Kim, J. Kang, J.Y. Noh, M.Y. Hyun, C. Kim, Y. Kim, S.-J. Kim, Novel Mn^{II} coordination compounds constructed from benzoate and various bipyridyl ligands: Magnetic property and catalytic activity, *Polyhedron*, **2012**, 42, 282–290.

98. N. de la Pinta, L. Fidalgo, G. Madariaga, L. Lezama, R. Cortés, Guest Driven Structural Correlations in DPDS [Di(4-pyridyl)disulfide]-Based Coordination Polymers, *Cryst Growth Des*, **2012**, 12, 5069–5078.

99. H.-L. Zhu, Y.-Q. Zheng, The synthesis, crystal structures, and thermal properties of a new Zn(II) coordination polymer with malonic acid, *Synthesis and Reactivity in Inorganic, Metal-Organic, and Nano-Metal Chemistry*, **2012**, 42, 736–740.

100. R.W. Seidel, C. Dietz, I.M. Oppel, Crystal structure of catena-[dichlorido-μ_2-4,4'-dithiodipyridine-κ2N:N'-zinc(II)], $C_{10}H_8Cl_2N_2S_2Zn$, *Zeitschrift Für Kristallographie - New Crystal Structures*, **2012**, 227, 305–306.

101. R.W. Seidel, C. Dietz, R. Goddard, I.M. Oppel, Non-merohedrally twinned catena-[dibromido-μ-4,4'-dithiodipyridine-κ2N:N'-zinc(II)], *J Chem Crystallogr*, **2013**, 43, 229–234.

102. N. de la Pinta, G. Madariaga, T. Ezpeleta, M. Luz Fidalgo, L. Lezama, R. Cortés, Spin canting in the $[Co_2(NCO)_4(DPDS)_4]\cdot 3H_2O$ [DPDS=di(4-pyridyl)disulfide] coordination polymer, *Polyhedron*, **2013**, 52, 1256–1261.

103. S. Sanda, S. Parshamoni, S. Konar, Third-generation breathing metal–organic framework with selective, stepwise, reversible, and hysteretic adsorption properties, *Inorg Chem*, **2013**, 52, 12866–12868.

104. A.B. Lago, R. Carballo, O. Fabelo, N. Fernández-Hermida, F. Lloret, E.M. Vázquez-López, Metallosupramolecular compounds based on Cu(II)/oxalate/twisted NSSN ligands showing a new in situ S–C bond cleavage, *CrystEngComm*, **2013**, 15, 10550-10562.

105. S. Sanda, S. Goswami, H.S. Jena, S. Parshamoni, S. Konar, A family of three magnetic metal organic frameworks: their synthesis, structural, magnetic and vapour adsorption study, *CrystEngComm*, **2014**, 16, 4742–4752.

106. H.-L. Zhu, J. Zhang, F.-Y. Yao, Y.-Q. Zheng, Copper(II), zinc(II), and cadmium(II) coordination polymers with 2-methylglutarato and 4,4′-dipyridyldisulfide, *Russian Journal of Coordination Chemistry*, **2014**, 40, 54–62.

107. Y.-H. Luo, Q.-L. Liu, Y. Ling, L.-J. Yang, W. Wang, B.-W. Sun, Guest molecules dependent structures, intermolecular interactions and magnetic properties of iron (II) polymer with 4,4′-dipyridyl disulfide, *Inorganica Chim Acta*, **2015**, 425, 255–259.

108. S. Sanda, S. Biswas, S. Parshamoni, S. Konar, Unraveling the multi-functional behavior in a series of Metal Organic Frameworks, *J Solid State Chem*, **2015**, 229, 103–111.

109. C.-C. Wang, G.-B. Sheu, S.-Y. Ke, C.-Y. Shin, Y.-J. Cheng, Y.-T. Chen, C.-H. Cho, M.-L. Ho, W.-T. Chen, R.-H. Liao, G.-H. Lee, H.-S. Sheu, A 3D

porous supramolecular architecture via π–π assembly of 2D metal–organic frameworks (MOFs): structure-versus-luminescence reversibility and gas adsorption properties, *CrystEngComm*, **2015**, 17, 1264–1272.

110. S. Sanda, S. Biswas, S. Konar, Study of proton conductivity of a 2D flexible MOF and a 1D coordination polymer at higher temperature, *Inorg Chem*, **2015**, 54, 1218–1222.

111. D. Sarkar, P. Chandra Rao, H.B. Aiyappa, S. Kurungot, S. Mandal, K. Ramanujam, S. Mandal, Multifunctional copper dimer: structure, band gap energy, catalysis, magnetism, oxygen reduction reaction and proton conductivity, *RSC Adv*, **2016**, 6, 37515–37521.

112. S.V.F. Beddoe, A.J. Fitzpatrick, J.R. Price, N. Mallo, J.E. Beves, G.G. Morgan, J.A. Kitchen, T.D. Keene, A bridge too far: testing the limits of polypyridyl ligands in bridging soluble subunits of a coordination polymer, *Cryst Growth Des*, **2017**, 17, 6603–6612.

113. A.A. Tehrani, H. Ghasempour, A. Morsali, A. Bauzá, A. Frontera, P. Retailleau, Unraveling the dual character of sulfur atoms in a series of Hg(II) coordination polymers containing bis(4-pyridyl)disulfide, *CrystEngComm*, **2017**, 19, 1974–1981.

114. S. Singha, A. Saha, S. Goswami, S.K. Dey, S. Payra, S. Banerjee, S. Kumar, R. Saha, A metal–organic framework to CuO nanospheres of uniform morphology for the synthesis of α-aminonitriles under solvent-free condition along with crystal structure of the framework, *Cryst Growth Des*, **2018**, 18, 189–199.

115. M. Mikuriya, R. Indrawati, R. Hashido, S. Matsubara, C. Nakamura, D. Yoshioka, K. Yokota, M. Fukuzaki, M. Handa, Chain Compounds based on

paddle-wheel copper(II) carboxylate bearing four nitroxide radicals, *Magnetochemistry*, **2018**, 4, 22.

116. X.-P. Sun, T. Liu, Z.-S. Yao, J. Tao, Spin crossover and photomagnetic behaviors in one-dimensional looped coordination polymers, *Dalton Transactions*, **2019**, 48, 9243–9249.

117. P. Daga, P. Majee, D.K. Singha, P. Manna, S. Hui, A.K. Ghosh, P. Mahata, S.K. Mondal, Dramatic luminescence signal from a Co(II)-based metal–organic compound due to the construction of charge-transfer bands with Al^{3+} and Fe^{3+} ions in water: steady-state and time-resolved spectroscopic studies, *New Journal of Chemistry*, **2020**, 44, 4376–4385.

118. P.-B. Zhu, Z.-L. Ke, H.-S. Won, S. Tan, A 2D Cu(II)-based coordination polymer: treatment effect on Parkinson's disease by increasing dopamine and VMA content, *Inorganic and Nano-Metal Chemistry*, **2020**, 51, 1331–1336.

119. T. Kanno, K. Nakabayashi, K. Imoto, S. Ohkoshi, Manganese-octacyanidoniobate-based ferrimagnet possessing bridging ligands with disulfide bonds, *Eur J Inorg Chem*, **2021**, 2021, 4681–4689.

120. P. Daga, P. Manna, P. Majee, D.K. Singha, S. Hui, A.K. Ghosh, P. Mahata, S.K. Mondal, Response of a Zn(II)-based metal–organic coordination polymer towards trivalent metal ions (Al^{3+}, Fe^{3+} and Cr^{3+}) probed by spectroscopic methods, *Dalton Transactions*, **2021**, 50, 7388–7399.

121. F. Zheng, L. Guo, R. Chen, L. Chen, Z. Zhang, Q. Yang, Y. Yang, B. Su, Q. Ren, Z. Bao, Shell-like xenon nano-traps within angular anion-pillared layered porous materials for boosting Xe/Kr separation, *Angewandte Chemie International Edition*, **2022**, 61, e202116686.

122. Y. Chen, D. Yang, Y. Wang, Q. Shi, B. Tang, C. Zhu, J. Li, L. Li, A robust metal–organic framework for simultaneous C_2H_4/C_3H_6 capture and C_2H_2/CO_2 separation, *Fuel*, **2024**, 368, 131673.

123. C.-C. Wang, P.-J. Liao, Y.-C. Chung, C.-Y. Shin, Y.-C. Wu, G.-H. Lee, S.-Y. Chien, B.-H. Chen, Y.-C. Chuang, Structural diversity and dimensionality of three Cu(II)-dpds-$C_5O_5^{2-}$ coordination polymers controlled by the coordination sphere of Cu(II) centers and the coordination modes of $C_5O_5^{2-}$ (dpds = 4,4′-dipyridyldisulfide), *ACS Omega*, **2024**, 9, 40920–40931.

124. M. Llunell, D. Casanova, J. Cirera, P. Alemany, S. Alvarez, SHAPE: Program for the Stereochemical Analysis of Molecular Fragments by Means of Continuous Shape Measures and Associated Tools, v2.1, Electronic Structure Group, Universitat de Barcelona. **2013**.

125. S. Alvarez, M. Llunell, Continuous symmetry measures of penta-coordinate molecules: Berry and non-Berry distortions of the trigonal bipyramid, *J. Chem. Soc., Dalton Trans.,* **2000**, 19, 3288–3303.